Deep-sea Research Part Ii-topical Studies In Oceanography
February 2018, Volume 148 Pages 151-179
https://doi.org/10.1016/j.dsr2.2017.05.006
https://archimer.ifremer.fr/doc/00385/49617/

Integrative species delimitation in the deep-sea genus *Thaumastosoma* Hessler, 1970 (Isopoda, Asellota, Nannoniscidae) reveals a new genus and species from the Atlantic and central Pacific abyss

Kaiser Stefanie [1, *], Brix Saskia [1], Kihara Terue C. [2], Janssen Annika [2], Jennings Robert M. [3]

[1] Senckenberg Meer, German Ctr Marine Biodivers Res DZMB, CeNak, Martin Luther King Pl 3, D-20146 Hamburg, Germany.
[2] Senckenberg Meer, DZMB, Sudstrand 44, D-26382 Wilhelmshaven, Germany.
[3] Temple Univ, Dept Biol, 1900 North 12th St, Philadelphia, PA 19122 USA.

* Corresponding author : Stefanie Kaiser, email address : stefanie.kaiser@senckenberg.de

Abstract :

Combined morphological and molecular analyses provided evidence for a new nannoniscid genus, Ketosoma gen. nov., including new species from abyssal waters of the equatorial NE Atlantic (eastern Vema Fracture Zone), SW Atlantic (Argentine Basin) as well as equatorial NE Pacific (Clarion Clipperton Fracture Zone, CCZ). Using mitochondrial (COI and 16S) and nuclear (18S) DNA markers together with morphological information from light scanning and confocal laser scanning microscopy we found clear differences between Ketosoma and its putative sister taxon Thaumastosoma Hessler, 1970. The new genus can be distinguished from the latter by the presence of a robust seta on pereonite 1 anterolateral corner and the lack of a ventral spine on the female operculum and pereonite 7 amongst others. Different species delimitation (SD) analyses were performed alongside morphological assessment to delineate species within Ketosoma. Here, four new species are described: Ketosoma vemae gen. et sp. nov. and K. hessleri gen. et sp. nov. from the eastern Vema Fracture Zone, K. werneri gen. et sp. nov. from the Argentine Basin and K. ruehlemanni gen. et sp. nov. from the CCZ. There is morphological and genetic evidence for the presence of at least two further Ketosoma species from the CCZ. Species within Thaumastosoma are reassessed; Thaumastosoma platycarpus Hessler, 1970 and T. tenue Hessler, 1970 are redescribed based on type material and the diagnosis updated accordingly. Furthermore, a new Thaumastosoma species, T. diva sp. nov., is described from the Argentine Basin. Thaumastosoma distinctum (Birstein, 1963) and T. jebamoni (George, 2001) are assigned to Ketosoma, with the latter species regarded as a nomen dubium.

Keywords : Molecular taxonomy, Vema-TRANSIT, DIVA 3, Clarion Clipperton Fracture Zone, Sexual dimorphism, Biodiversity, Janiroidea, Deep sea

1. Introduction

The abyssal seafloor, usually defined as areas between 3000 and 6000 m depth, represents the largest benthic environment on Earth covering more that 50% of its surface (Gage and Tyler, 1991). Contrary to earlier perceptions though, abyssal areas are not homogeneous and flat, but reveal considerable spatial and temporal variation related to depth, surface productivity, geomorphology and current regimes - amongst others. In some areas - mainly in the central Pacific and Indian oceans - manganese nodules form large deposits and can locally increase habitat complexity (e.g., Janssen et al., 2015), while mid-ocean ridges can form important biogeographic barriers (McClain et al., 2009; but see Brix et al., 2011; Havermans et al., 2013; Brandt et al., this issue). The variety of habitats and related conditions at abyssal depth support a highly diverse yet still poorly known benthic fauna (Tyler et al., 2016). Inevitably every abyssal sample taken yields a high proportion of species new to science and also has the potential to increase the number of supra-specific taxa by improving current phylogenies (Mora et al., 2011; Riehl et al., 2014b; Brix et al., 2015).

Species delimitation is the initial step to describe biological diversity. Defining thresholds to delineate species and higher taxonomic ranks is challenging though especially in the deep sea, where

individual numbers are too low to sufficiently capture intraspecific variability (Brandt et al., 2007; Lim et al., 2012). Furthermore, cryptic species that lack morphological differentiation, but differ genetically are widespread leading to an underestimation of true species richness (Etter et al., 2005; Raupach et al., 2007; Havermans et al., 2013). In contrast, strong sexual dimorphism, where males and females show significant morphological variation, makes allocation of conspecifics difficult and males and females may even be assigned to different species (Riehl et al., 2012; Blazewicz-Paszkowycz et al., 2014). There is now a trend towards using a combined morphological and genetic approach to the taxonomy of deep-sea taxa making demarcation of species boundaries more robust (e.g., Havermans et al., 2013; Brandt et al., 2014; Brix et al., 2015).

Asellotan isopods are a ubiquitous and particularly rich component of the deep-sea fauna, typically comprising more than 90% of total isopod specimens (Wilson, 1998; Brandt et al., 2007; Brix et al., this issue). Of the 25 extant marine asellotan families, 19 have representatives in the abyss, some of which have been almost exclusively found in the deep sea (Merrin, 2014; Schotte et al., 2009). For some asellotan lineages an ancient deep-sea origin has been suggested; there is evidence that ancestors of the so-called munnopsoid radiation (e.g. Munnopsidae, Desmosomatidae and Nannoniscidae) have evolved *in situ* during the Carboniferous/Triassic (between 232 and 314 Myr ago) enduring several past anoxic periods (Wilson, 1999; Raupach et al., 2004; Lins et al., 2012).

The family Nannoniscidae has a wide distribution in the deep sea, yet some species have been recorded from shelves at high northern and southern latitudes (Kaiser et al., 2009; Brix and Svavarsson, 2010). So far, 80 formally described species in 12 genera are known from most major oceans ranging from the Mediterranean, Atlantic, Pacific, and Arctic oceans to the Southern Ocean (Kaiser, 2014, 2015; Schotte et al., 2009). Although no nannoniscid has been described from the Indian Ocean to date, this is likely to reflect undersampling and the family is thus presumed to have a cosmopolitan distribution.

During recent deep-sea expeditions specimens of new nannoniscid species were discovered in the North Atlantic (Vema Fracture Zone), South Atlantic (Argentine Basin) as well as in the central equatorial Pacific (Clarion Clipperton Fracture Zone, CCZ). These species show strong resemblance to *Thaumastosoma* Hessler, 1970, but do not fit into the current classification, and are therefore assigned to a new genus within the Nannoniscidae. We carried out a molecular phylogenetic analysis of of three DNA markers (COI, 16S and 18S). We applied five different species delimitation (SD) methods of molecular data to delineate species within *Thaumastosoma* and the new genus (i.e., General Mixed Yule Coalescent [GMYC], bPTP, STACEY, BPP, and Automatic Barcoding Gap Discovery [ABGD]; Pons et al., 2006; Yang and Rannala, 2010; Puillandre et al., 2012; Rannala and Yang, 2013; Zhang et al., 2013; Jones et al., 2014) and compared results with findings from morphological examination. Following on from this, we provide a description of a new nannoniscid genus including five new species. Furthermore, species (type specimens) within *Thaumastosoma* were reassessed and the diagnosis amended in the light of these new findings.

2. Material and methods

2.1 Sampling and sample processing

Samples were obtained during recent deep-sea expeditions to the North and South Atlantic as well as equatorial Pacific (CCZ) (Table 1; Devey, 2015). A distribution map was produced in QGIS (QGIS, 2015; see Fig. 1). Sampling was conducted using an epibenthic sledge (EBS *sensu* Brenke, 2015), a C-EBS and a Rothlisberg & Pearcy sled (RP sledge) respectively (Kaiser and Brenke, 2016). For a full list of stations and related metadata see Table 1. On-board, the samples were elutriated and sieved (through a 300 µm mesh) in cold seawater, then fixed in pre-cooled (-20°C) 96% pure ethanol and kept at -20°C for at least 48 hours (VEMA: 24h). After 24 hours (VEMA: 12h) samples were re-fixed with 96% ethanol to ensure preservation of high-quality DNA and kept at -20°C until further sample processing (Riehl et al., 2014a). Samples were sorted on board to family level and in the laboratories of the German Centre for Marine Biodiversity Research (DZMB, Wilhelmshaven and Hamburg, Germany) to lowest taxonomic resolution.

2.2 Morphological methods

Appendages were dissected and partly mounted in methylene green stained glycerine gelatine respectively. For species, where only one specimen was present, most appendages were drawn *in situ* or only dissected from one side (mouthparts) to keep the holotype intact. Illustrations were made using Leica DMLS and DM 2500 microscopes with a camera lucida. Assessment of length-width ratios and the terminology follows methods proposed by Hessler (1970). The terminology of setation follows Wolff (1962), Hessler (1970) and Riehl and Brandt (2010). The material is deposited at the Zoological Museum of Hamburg (ZMH). The article is registered in ZooBank under urn:lsid:zoobank.org:pub:0688957A-81BA-49B0-A597-7768A4F0583E.

Confocal Laser Scanning Microscopy (CLSM)

Eight specimens were used for CLSM as indicated in the descriptions below: 1 adult male specimen (voucher No. NBIso337, ZMH K 46139, Table 2), 1 adult male specimen (VTDesm013, ZMH K 46140), 1 ovigerous female specimen (VTDesm569, ZMH K 46141), 1 adult male specimen (D3D064, ZMH K 46132), 1 ovigerous female specimen (D3D060, ZMH K 46142), as well as 2 specimens of *Thaumastosoma platycarpus* Hessler, 1970 *(*1 ovigerous female, 1 adult male, Australian Museum, P.59254) and 1 ovigerous female of *Thaumastosoma tenue* Hessler, 1970 (Australian Museum, P.59256). Prior to the dissection of appendages specimens were stained with 1:1 solution of Congo Red and Acid Fuchsin overnight using procedures adapted from Michels and Büntzow (2010). The whole specimen was temporarily mounted onto a slide with glycerine, and self-adhesive plastic reinforcement rings were used to support the coverslip (Kihara and Rocha, 2009; Michels and Büntzow, 2010). To mount the specimens in lateral view, Karo® light corn syrup was used as mounting medium (Kihara et al., in preparation) and double sided tape pieces were combined in appropriate thickness, between the slide and coverslip, so that the body was not compressed. The material was examined using a Leica TCS SP5 equipped with a Leica DM5000 B upright microscope and 3 visible-light lasers (DPSS 10 mW 561 nm; HeNe 10 mW 633 nm; Ar 100 mW 458, 476, 488 and 514 nm), combined with the software LAS AF 2.2.1. (Leica Application Suite Advanced Fluorescence). Images were obtained using objective HCX PL APO CS 10.0x0.40 DRY UV and 561 nm excitation wavelength with 80% acousto-optic tunable filter (AOTF). Series of stacks were obtained, collecting overlapping optical sections throughout the whole preparation with optimal number of sections according to the software. The acquisition resolution was 2048×2048 pixels and the settings applied for the preparations are given in Table 3. Final images were obtained by maximum projection, and CLSM illustrations were composed and adjusted for contrast and brightness using the software Adobe Photoshop CS4.

2.3 Molecular-genetic methods

DNA extraction, PCR amplification, and sequencing

DNA extraction and PCR amplification was conducted at Senckenberg Institute (DZMB) in Wilhelmshaven and at the Laboratories of Analytical Biology, Smithsonian Institution (USNM), Washington, D.C. USA. At DZMB, DNA was extracted from 1 to 3 posterior legs of three specimens (voucher No. NB12_Iso740_9, KM14 Iso259_1 and KM14Iso261_2, see Table 2) following Janssen et al. (2015). The remaining specimens were analysed at USNM. Here, DNA was extracted from one posterior leg of each specimen using protocols described in Brix et al. (2011) and Riehl et al. (2014a). Separate PCR reactions were conducted for the nuclear small ribosomal subunit (18S) and for mitochondrial cytochrome c oxidase subunit I (COI) and large subunit (16S). Primers and PCR protocols were as described in Riehl et al. (2014a). Amplified PCR products were purified for sequencing using ExoSap-IT (USB), and bidirectionally sequenced using standard BigDye chemistry (Perkin-Elmer) on an ABI 3730xl capillary sequencer. For specimens analyzed at DZMB, PCR-

products were purified in the same way and sent to the Macrogen Europe Laboratory in Amsterdam, Netherlands for sequencing using the same set of primers as used for the PCR. For each sequenced individual, both strands of each gene were aligned in Geneious 9.1.6 and disagreements were resolved by hand. Alignments of 18S and 16S were made with the online MAFFT server v7 (Katoh and Standley 2013) and ambiguously aligned portions of the alignment were removed using the online Gblocks server (Talavera and Castresana, 2007), employing all three criteria for less-stringent selection. Alignment of DNA sequences of COI was performed on translated amino acids using the Clustal X algorithm (Larkin et al., 2007) as implemented in BioEdit. All alignments were edited for consistency by hand, and ends were trimmed to avoid large blocks of gaps. Furthermore, a published sequence of COI for one species (voucher No. NBIso337) of the new genus was obtained from GenBank (Table 2). Where subsequent analyses required an outgroup (see below), published sequences of 18S, 16S, and COI of three species of *Chelator* were obtained from GenBank (Table 2) and included in alignment and trimming steps. All new sequences generated in this work were deposited in GenBank (see Table 2).

Species delimitation analyses

Several species delimitation (SD) analyses were conducted, including both "discovery" and "validation" methods (e.g., Carstens et al., 2013). While some SD algorithms use sequences as input, most either use a fixed phylogenetic tree or require one as a guide tree; therefore, BEAST2 v.2.4.4 (Bouckaert et al., 2014) was used to estimate the single best Bayesian phylogeny from the 18S, 16S, and COI alignment including the *Chelator* outgroup. Each alignment was treated as a separate partition with its own mutational model. The COI partition was given four categories of gamma-distributed rate variation with estimated shape parameter, and an HKY model of mutation with mean rate set to 1; the 16S and 18S partition was also given gamma-distributed rate variation, but with a GTR model of mutation whose mean mutation rate was estimated relative to COI. All partitions shared a single log-normally distributed molecular clock for branch length optimization (Drummond et al., 2006). All default gamma priors were changed to lognormal priors, and all 1/X priors were changed to exponential priors. Convergence of the BEAST2 run was assessed with Tracer v1.6 (Rambaut et al., 2014) to ensure that all ESSs were ≥200. The branching patterns obtained in this multilocus tree were used in SD analyses where a guide tree was needed. Each locus was also used individually, with the same options as above, to estimate the best locus-specific tree. These single locus trees (with branch lengths) were used in some SD analyses as discussed below and are included in the supplementary material, Figs S1–3.

Four "discovery" SD algorithms were employed: Automatic Barcode Gap Discovery (ABGD, Puillandre et al., 2011), the General Mixed Yule Coalescent (GMYC; Pons et al., 2006), its relative bPTP (Zhang et al., 2013), and the STACEY algorithm (Jones et al., 2014). The "validation" algorithm BPP (Bayesian Phylogenetics and Phylogeography, Yang and Rannala, 2010; 2013) was used as an independent assessment of the delimitations produced by the discovery methods and those supported by morphology. For GMYC and bPTP, the BEAST2 single-locus gene trees with branch lengths were uploaded to online servers and SD analysis employed standard options; the GMYC analysis was run with both single and multiple species thresholds. STACEY analysis was conducted on the partitioned 3-locus dataset in BEAST2 following the tutorial, employing the same DNA mutation models as in phylogenetic tree estimation, the default Yule prior, and changes to gamma and 1/X priors as above. After ensuring convergence of the run, assessment of species partitions was performed with the "speciesDA.jar" program in the STACEY package. Finally, the BPP algorithm was employed to obtain posterior support values for species delimitations produced by the discovery methods, using the multilocus tree as the fixed guide tree. A theta prior with parameters 2 and 200 was employed, and a tau prior with parameters 30 and 1000; the algorithm was run with both delimitation models described in Yang and Rannala (2010).

2.4 Comparative material

For comparison, the following type material was requested from the United States National Museum Smithsonian Institution (USNM), and the Australian Museum, Sydney:

USNM 125112, *Thaumastosoma platycarpus*, holotype, female
Australian Museum, P.58793, *Thaumastosoma platycarpus*, paratype, 1 manca
Australian Museum, P.59254, *Thaumastosoma platycarpus* paratypes, 1 male, 3 females
Australian Museum, P.59254, *Thaumastosoma platycarpus* paratypes, 1 male for CLSM
Australian Museum, P.59254, *Thaumastosoma platycarpus* paratypes, 1 female for CLSM
Australian Museum, P.65517, *Thaumastosoma platycarpus*, paratypes, 3 mancas
USNM 125113, *Thaumastosoma tenue*, holotype, female
Australian Museum, P.59255, *Thaumastosoma tenue*, paratype, 1 female
Australian Museum, P.59256, *Thaumastosoma tenue*, *paratype*, 1 female for CLSM and illustration of mouthparts
USNM 138731, *Prochelator sarsi*, holotype, female
USNM 138732, *Mirabilicoxa hessleri*, holotype, male
USNM 138733, *Mirabilicoxa alberti*, holotype, female

Remarks. An adequate effort was made to procure and examine described species within *Thaumastosoma sensu lato*. We were not able though to allocate the type material of *Thaumastosoma jebamoni* (George, 2001). In his paper, George (2001) assigned the same catalogue number to holotypes of three species (i.e., *Mirabilicoxa alberti* George, 2001, *Eugerda svavarssoni* George, 2001 and *Thaumastosoma jebamoni* (George, 2001)). For clarification, we ordered all type specimens listed in George (2001) and assigned to a catalogue number. However, when investigating the material we found only the holotype of *M. alberti* being present whereas the holotypes of *T. jebamoni* and *E. svavarssoni* were missing (see also Wilson, 2008). Thus, both species must be regarded as a nomen dubium (Wilson, 2008). Furthermore, we made a sufficient attempt to allocate the type material of *Thaumastosoma distinctum* (Birstein, 1963), which, however, is currently not available due to re-organisation of the museum collections (K. Minin, pers. communication).

2.5 Abbreviations

In the taxonomic descriptions and figure legends the following abbreviations were used: A1—antennula, A2—antenna, lMd—left mandible, rMd—right mandible, Mx1—maxillula, Mx2—maxilla, Mxp—maxilliped, Op–operculum, PI–PVII—pereopods I–VII, Plp 1–5—pleopods 1–5, Plt—pleotelson

3. Results

3.1 Morphological assessment

During recent expeditions several morpho-types were discovered that show strong resemblance to species within *Thaumastosoma*, for example, in having the mouthparts forwardly produced, the maxilliped bearing unusually long coupling hooks, the robustness of pereopod I compared to pereopod II, as well as the triangular shape of pereopod I carpus (cf. Hessler, 1970; Wilson, 2008; Riehl et al., 2014b). In *Thaumastosoma* Hessler, 1970 there are currently four species described from the bathyal and abyssal of the Northern Atlantic and Pacific oceans (cf. Wilson, 2008), viz.: *T. distinctum* (Birstein, 1963), *T. jebamoni* (George, 2001) nomen dubium, T. *platycarpus* Hessler, 1970 and *T. tenue* Hessler, 1970. However, morphological examination revealed clear differences between a cluster formed by three *Thaumastosoma* species (*T. platycarpus* and *T. tenue*, *Thaumastosoma* sp. nov., described below) and four new species (described below) together with *T. jebamoni* and *T. distinctum*. The latter cluster can be distinguished from *Thaumastosoma sensu stricto* as follows: seta present on the anterolateral corner of the first pereonite (seta present on the coxa in *Thaumastosoma*

species), absence of a ventral spine on pereonite 7 and the female operculum (ventral spine present) as well as maxilla mesial endite more than half of the remaining endites (mesial endite ≤ 0.5 times lateral and middle endite length). Furthermore the number of antennula articles is ≥ 11 in most species belonging to this cluster, which is quite unusual for any nannoniscid species.

As described above, the status of *T. jebamoni* is problematic; the species was first described by George (2001) to erect the monotypic genus *Leutziniscus*. A type species was not designated in the original description by George (2001), but Wilson (2008) denotes *T. jebamoni* by monotypy (see ICZN Article 68.3). However, Wilson (2008) did not find any apomorphies to distinguish *Leutziniscus* from *Thaumastosoma* and therefore regarded *Leutziniscus* as a junior synonym for *Thaumastosoma* Hessler, 1970 (cf. Wilson, 2008). As the holotype of *T. jebamoni* is missing, the species should be regarded as a nomen dubium (Wilson, 2008). We therefore do not re-establish *Leutziniscus*, but erect a new genus, *Ketosoma* gen. nov.; this is because the type species of *Leutziniscus* represents a *nomen dubium and* generic features cannot be adequately inferred on the basis of illustrations provided by George (2001). Furthermore investigations of the new species revealed a number of additional characters present in the new species but not mentioned in the description of *Leutziniscus*. These, however, are important diagnostic features to distinguish them from the remaining *Thaumastosoma* species; for instance, in *T. jebamoni* there is neither a seta shown on the coxa nor the anterolateral margin of the first pereonite. Furthermore, the maxilla is not illustrated in *T. jebamoni*.

3.2 Species delimitation analyses

The PCR success was low (67%, 47%, and 27% for 16S, 18S, and COI respectively), which however is not unusual for small data sets (Brix et al. 2011), so not all three genes were covered for all examined specimens (Table 2). Yet, multilocus Bayesian phylogenetic analysis generated reasonable support when all three genes were used in concert to create a multilocus tree.

The multilocus phylogenetic tree (Fig. 2) showed strong support for a deep split among specimens, defining a clade of *Thaumastosoma sensu stricto* and a clade of *Ketosoma* (1.0 Bayesian posterior probability (PP) in all cases). Likewise within the *Ketosoma* clade, there was strong support for phylogenetic separation of three Pacific specimens (KM14_Iso259_1, KM14_Iso261_2, NB12_Iso740_9; Fig. 2) from all others (0.90-1.0 PP). In general, the presence of deep and shallow branches in both subclades made SD analysis especially pertinent.

The three discovery SD analyses produced largely congruent species groups that received high support by the BPP validation method (Fig. 2). All discovery methods grouped IDesm010, 012, 041, 045, and 046 (all *T.* cf. *platycarpus)* into a single species; the GMYC with multiple species threshold added D3D064 (*Thaumastosoma* sp. nov.) to this species, while all other methods delineated it as a separate species (0.99 BPP support for inclusion vs. 0.76 support for exclusion). Likewise, in the *Ketosoma* clade all discovery methods grouped KM14_Iso259_1 and KM14_Iso261_2 into a single species, with NB12_Iso740_9 included in half of the SD determinations (0.99 BPP support for inclusion vs. 0.39 support for exclusion). In the *Ketosoma* clade, most delimitation methods kept all remaining specimens as separate species, though only NBIso337 was separate in 100% of SD analyses. ABGD analysis at 16S detected a barcode gap between 1% and 4% pairwise difference (Table 4); because only COI sequences were obtained for four specimens, there were too few pairwise comparisons for ABGD on COI (Table 5).

In accordance with the SD analyses of the molecular data, the new genus includes six new species from the North and South Atlantic, as well as equatorial North Pacific, of which four are described below. Furthermore, it reveals a new species of *Thaumastosoma* from the Argentine Basin (see description below). Here, *T. jebamoni and T. distinctum* are transferred to *Ketosoma* although characters do not entirely fit the diagnosis and/or could not be inferred from the illustrations provided by Birstein (1963) and George (2001); yet they share a number of diagnostic and apomorphic features with species in the new genus (Table 6, see also discussion below): lack of a ventral spine on the female operculum; presence of well developed posterolateral spines in female (both species); robust seta present on the anterolateral corner of the first pereonite (*K. distinctum comb. nov*.); antennula

article with ≥11 articles (*K. jebamoni* comb. nov.). So, for now these species should be placed in *Ketosoma* until further examination of type specimens and/or newly collected material.

3.3 Taxonomy

Suborder Asellota Latreille, 1803
Suprafamily Janiroidea Sars, 1897
Family Nannoniscidae Hansen, 1916
Desmosomidae Sars, 1899: 118; Vanhöffen, 1914: 549; Nannoniscini Hansen, 1916: 83; Nannoniscidae Siebenaller & Hessler, 1977: 17–43.

Type genus: *Nannoniscus* Sars, 1870

Composition: *Austroniscus* Vanhöffen, 1914; *Exiliniscus* Siebenaller & Hessler, 1981; *Hebefustis* Siebenaller & Hessler, 1977; *Ketosoma* Kaiser & Brix gen. nov.; *Micromesus* Birstein, 1963; *Nannoniscoides* Hansen, 1916; *Nannonisconus* Schultz, 1966; *Nannoniscus* Sars, 1870; *Nymphodora* Kaiser, 2008; *Panetela* Siebenaller & Hessler, 1981; *Rapaniscus* Siebenaller & Hessler, 1981; *Regabellator* Siebenaller & Hessler, 1981; *Thaumastosoma* Hessler, 1970.

***Thaumastosoma* Hessler, 1970**
Thaumastosoma Hessler, 1970: 25; George, 2001: 1843; Wilson, 2008: 9.

Type species: *Thaumastosoma platycarpus* Hessler, 1970

Species included (see also Table 7): *Thaumastosoma platycarpus* Hessler, 1970; *T. tenue* Hessler, 1970**;** *T. diva* Kaiser & Jennings sp. nov.

Diagnosis (modified after Hessler, 1970). A1 with 6 articles. Mouthparts produced conspicuously forward. Md elongate, incisor process bent forward, lacinia mobilis membranous, palp well developed. Mxp with unusually elongate coupling hooks, palp segments 2–4 produced forward medially. Mesial endite of Mx2 less than half the length of the other endites, with 1 long slender seta and several somewhat smaller ones. PI more robust than PII. Pereonite 1 somewhat larger than pereonite 2. Coxae of PI slightly produced, each tipped with a robust seta, anterolateral margins of pereonites 2–4 each with a robust seta. A ventral spine present on pereonite 7 and female Op. Urp biramous. Sexual dimorphism modest; in copulatory male Plt broader posteriorly, with acute posterolateral spines, in female Plt with pair of very poorly developed posterolateral angularities.

***Thaumastosoma platycarpus* Hessler, 1970** (Figs 3–4)
Material examined. Holotype: 1 female holotype (preparatory), USNM 125112. Paratypes: 1 manca, Australian Museum, P.58793; 1 male, 3 females, Australian Museum, P.59254; 1 male (adult) and 1 female (ovigerous) for CLSM, Australian Museum, P.59254; 3 mancas, Australian Museum, P.65517.

Redescription of paratype female. *Habitus* (Fig. 3a–d). Body length 5.1 pereonite 2 width. Coxae 1 visible in dorsal view. Pereonite 7 and Op each with a strong ventral spine (Fig. 3b–d). Pereonites 2–4 decreasing in width. Pereonite 1 widest (damaged). Pereonite 1 length 1.3 pereonite 2 length. Pereonites 2–4 of similar length. Pereonites anterior margins 1–4 frontally directed, rounded. Pereonite 1 coxae each with a robust spine; anterior lateral tergites of pereonites 2–4 each tipped with a small robust seta. Pereonites 5 width 0.9 pereonite 2 width. Pereonite 5 longest, length 1.8 pereonite 2 length, width 1.1 pereonite 4 width. Pereonite 5 and 7 anterior margins slightly concave, pereonite 6 anterior margin straight. Plt length 0.2 body length, length 0.9 width, with a pair of very poorly developed posterolateral angularities; Plt width 0.9 pereonite 2 width, posterior margin strongly

rounded, anterior margin slightly concave. Anus (Fig. 3d) covered by anus valves laterally. Urp inserting closely to the anus valves, length 0.5 Plt length, projecting beyond posterior margin.

Cephalothorax (Fig. 3a–b). Free, almost as long as wide. Anterior, posterior and lateral margins slightly rounded. Transition of frons, clypeus, and labrum smooth, without transverse ridge; clypeus and labrum extending 0.2 beyond frontal margin. Antennae inserting frontolaterally in a deep fold.

Redescription of paratype male. *Habitus* (Fig. 4a–d). Body length 4.8 pereonite 2 width. Coxae 1 visible in dorsal view. Body gradually flattening from pereonite 1 to 4 and increasing in height from pereonite 5 to 7. Pereonite 3, 4 and 7 each with a distinct ventral spine (Fig. 4b–d). Pereonites 1 to 4 decreasing in width. Pereonite 1 widest, length 0.3 width. Pereonite 2 width 0.9 pereonite 1 width, length 0.8 pereonite 1 length. Pereonites 2–4 of similar length. Pereonites anterior margins 1–4 frontally directed, rounded. Pereonite 1 coxae each with a robust spine; anterior lateral tergites of pereonites 2–4 each tipped with a small robust seta. Pereonite 5 longest, length 1.7 pereonite 1 length, about as wide as pereonite 1 width, width 1.3 pereonite 4 width. Pereonite 5 anterior margin concave, pereonite 6–7 anterior margins straight. Plt length 0.2 body length, length 0.8 width, Plt width 0.9 pereonite 1 width, with a pair of well-developed posterolateral spines, posterior margin almost straigtht, anterior margin concave. Anus (Fig. 4d) covered by anus valves laterally. Urp inserting closely to the anus valves, length 0.4 Plt length, projecting beyond posterior margin.

Cephalothorax (Fig. 4a–b). Free, length 0.9 width. Anterior, posterior and lateral margins slightly rounded. Transition of frons, clypeus, and labrum smooth, without transverse ridge (Fig. 4b). Antennae inserting frontolaterally in a deep fold.

Remarks. The CLSM images revealed some additional features not documented in Hessler's (1970) description. These mostly refer to the presence of ventral spines on pereonites 3 and 4, which seems to be a dimorphic character only occurring in the male specimen. Other gender-related characters include: pereonite 5 wider in male (width 1.3 pereonite 4 width vs. 1.1); pereonite 4 tapering in male (rectancular in female); width 1.4 pereonite 4 width (female 1.3); Plt quadrangular (Plt tapering in female towards anterior end); posterolateral spines well developed in male (only poorly developed in female). Furthermore the antenna is swollen in male (i.e., peduncular articles 5, 6 and flagellar articles), yet no A2 is known for the female.

***Thaumastosoma tenue* Hessler, 1970** (Figs 5–6)

Material examined. Holotype: 1 female holotype (preparatory), 4 mm, USNM 125113. Paratypes: 1 paratype female (damaged), Australian Museum, P.59255; 1 female, ovigerous, for CLSM and illustration of mouthparts, Australian Museum, P.59256.

Remarks. A redescription of certain features of *T. tenue* is necessary as some important characters (e.g. habitus, Mx2) were not illustrated by Hessler, 1970.

Redescription holotype and paratype female. *Habitus* (Figs 5a, c, 6a–c), body length 4.7 pereonite 2 width. Coxae 1 and 4 visible in dorsal view. Body gradually flattening from pereonite 1 to 4 and decreasing in height from pereonite 5 to 7. Pereonite 7 and Op each with a strong ventral spine (Figs 5c, 6b, c). Pereonites 2–4 decreasing in width. Pereonite 2 widest, length 0.3 width. Pereonite 1 width 0.9 pereonite 2 width, length 1.1 pereonite 2 length. Pereonites 2 and 3 of similar length; pereonite 4 length 1.2 pereonite 2 length. Pereonites 1–4 anterior margins frontally directed, rounded. Pereonite 1 coxae each with a robust seta; anterior lateral tergites of pereonites 2–4 each tipped with a small robust seta. Pereonites 5 width 0.8 pereonite 2 width. Pereonite 5 longest, length twice pereonite 2 length, width 1.1 pereonite 4 width. Pereonite 5 anterior margin straight, pereonite 6 anterior margin convex,

pereonite 7 anterior margin straight. Plt length 0.2 body length (measured from lateral view), about as long as wide, width 0.9 pereonite 1 width, with a pair of poorly developed posterolateral angularities inserting 0.8 from anterior margin; posterior margin straight, anterior margin concave. Anus (Fig. 6c) covered by anus valves laterally. Urp inserting closely to the anus valves, length 0.4 Plt length, projecting beyond posterior margin.

Cephalothorax (Figs 5a–c, 6b). Free, almost as long as wide. Anterior, posterior and lateral margins slightly rounded. Transition of frons, clypeus, and labrum smooth, without transverse ridge (Fig. 5b); clypeus and labrum extending 0.2 beyond frontal margin. Antennae inserting frontolaterally in a deep fold.

LMd (Fig. 5d–e). Md palp well developed, consisting of 3 articles, reaching mid incisor. Palpal article 1 length 0.9 article 2 length, with 1 long simple seta distally. Article 2 with 2 simple setae medially and several small setae laterally. Terminal article length about one-third article 2 length, tapering distally, with 6 small setae ventrally and 2 more robust setose setae terminally. Incisor process with 4 teeth, subdistal tooth reduced. Lacinia mobilis blunt. Setal row with 10 robust dentate setae of varying size and several slender setae in between, with 6 long simple setae proximally. Molar process triangular, with 12 long, serrate setae distally.

Mx2 (Fig. 5f). Outer margins of mesial endite with 1 long slender seta and several somewhat smaller setae. Mesial endite reduced, length 0.4 lateral endite. Lateral and middle endites each with 4 strong setae distally.

***Thaumastosoma diva* Kaiser & Jennings sp. nov.** (Figs 7–8)

Type fixation: Holotype, adult male, designated here.

Material examined. Holotype: 1 adult male, 1.7 mm (measured without Plt), Argentine Basin, SW Atlantic, DIVA-3 expedition, RV Meteor, EBS, station 534 (start: 36.01016’S, 49.02566’W; end: 36.0115’S, 49.029’W, 4608 m), date: 16/07/2009, voucher No. D3D064, ZMH K 46132.

Etymology. *Diva* is female and relates to the sampling campaign (DIVA - DIVersity of the abyssal Atlantic Ocean) during which the species was collected.

Distribution. Argentine Basin, SW Atlantic, 4608 m; only known from the type locality.

Diagnosis. A2 with 6 peduncular and 23 flagellar articles in male; pereonites 3–4 without ventral spine; coxae of pereonite 1 and anterolateral margins of pereonites 2–4 each with a very robust spine; coxa 1 spine length half pereonite 1 length.

Description of holotype male. *Habitus* (Figs 7a, 8a–c) Plt broken off. Coxae of pereonite 1 visible in dorsal view. Pereonites 2–4 and 5–7 decreasing in width; pereonite 5 widest, width 1.2 pereonite 4 width, length 0.6 width. Pereonite 1 width 0.9 pereonite 5 width, length 0.4 width. Pereonites 2 width almost as wide as pereonite 5. Pereonites 2–4 of similar length, length 0.8 pereonite 1 length. Pereonites 1–4 anterior margins frontally directed, rounded. Pereonite 1 coxae each with a robust spine, length half pereonite 1 length; anterior lateral tergites of pereonites 2–4 each tipped with a robust seta. Pereonite 5 longest, length 1.8 pereonite 1 length. Pereonite 5 and 6 anterior margins straight.

Cephalothorax (Figs 7a, 8a–d). Free, wider than long. Anterior and frontal margins strongly rounded, posterior margin slightly rounded. Mouthparts not visible from dorsal view. Antennae inserting frontolaterally in a deep fold.

A1 (Fig. 7b, 8a–d*)*, drawn *in situ*. With 6 articles. First article rectangular and broadest, length 1.9 width, with 2 broom setae of varying size distally. Second article length 1.2 article 1 length, length 3.3 width, with 4 broom setae of varying size distally. Article 3 length 0.6 article 2 length, with 1

simple seta distally. Article 4 length 0.3 article 2 length, with 1 small broom seta distally. Article 5 length 0.3 article 2 length. Article 6 length about half article 2 length, with 3 long slender simple setae, 1 small broom seta and 1 terminally.

A2 (7a, b, 8c), from CLSM. With 6 peduncular and 23 flagellar articles. Peduncular articles 1–4 short. Article 3 with 1 robust unequally bifid seta, 1 small spine and 1 simple seta; article 4 with 1 simple seta distally. Articles 5–6 long and slender. Article 5 with robust unequally bifid setae laterally. Flagellar articles 1–13 indistinctly separated from each other, lacking any setae, marcation between articles 14–23 more distinct.

Mx2 (Fig. 7d). Outer margin of mesial endite with several setae of varying length, with 1 long slender seta and several somewhat smaller setae. Mesial endite reduced, length 0.4 lateral endite. Lateral and middle endites each with 4 strong setae distally.

PI (Fig. 7c). Basis length 6.6 width, with 2 simple setae and 1 broom seta dorsally, with 2 setae (1 simple 1 broken off) ventrally, with 2 long strong simple setae distoventrally. Ischium about half basis length, length about twice width, with 2 setae (1 simple, 1 broken off) ventrally. Merus length half ischium length, length 1.2 width, with 2 long robust simple setae distodorsally, 2 simple setae ventrally. Carpus length twice merus length, length 2.6 width, with a row of 4 simple setae dorsally, with numerous small setae, membranously embedded, and with 5 unequally bifid setae in between. Propodus length 0.75 carpus length, length 3.6 width, with 2 simple setae dorsally, with 1 small unequally bifid seta and 1 simple seta distoventrally. Dactylus length 0.7 propodus length, length 4.8 width, with 3 slender setae medially. Unguis length one-third dactylus length, with 2 long, slender setae between unguis and ventral claw.

Plp 1 (Figs 7e, 8b), from CLSM. Length 2.4 proximal width. Distal projection width 0.6 proximal width, lateral margins straight. Lateral lobes elongate, rounded; distal margins strongly rounded, with 7 simple setae of varying length each.

Remarks. *T. diva* sp. nov. is most similar to *T. platycarpus*, but can be distinguished from the latter as follows: ventral spines absent from pereonites 3 and 4 (vs. ventral spines present in *T. platycarpus*); coxa 1 spine length half pereonite 1 length (vs. 0.3 pereonite 1 length); pereonite 5 anterior margin straight (vs. strongly concave). Distinguishing *T. diva* from *T. tenue* is complicated by the fact that for the latter species only the female is known. Thus, potential differences may arise from sexual dimorphism. From comparing both sexes in *T. platycarpus* (see summary above), characters that are more or less conservative between male and female include for instance the antennula, as well as pereopods, but also length of spines on coxa 1 as well as length/width ration of the tergites of pereonites 2–4. Accordingly *T. diva* differs from *T. tenue* as follows: A1 article 6 length > article 5 length (vs. article 6 length < article 5 length) coxa 1 spine length half pereonite 1 length (vs. 0.2 pereonite 1 length in *T. tenue*); PI overall less setose and more slender in *T. diva*; PI basis with 2 simple setae and 1 broom seta dorsally (vs. 9 small simple setae); PI merus with 2 simple setae ventrally (vs. 7 setae ventrally); PI carpus more than twice width (vs. less than twice width).

***Ketosoma* Kaiser & Brix gen. nov.**

Desmosoma G.O. Sars, 1864*; Birstein, 1963: 121; Leutziniscus George, 2001: 1844; Thaumastosoma* Hessler, 1970*: 19; Wilson, 2008: 10.*

Type species: *Ketosoma ruehlemanni* gen. et sp. nov., by original designation

Species included (see also Table 7): *K. distinctum* (Birstein, 1963), comb. nov.; *K. hessleri* gen. et sp. nov.; *K. jebamoni* (George, 2001), comb. nov. (nomen dubium); *K. ruehlemanni* gen. et sp. nov.; *K. vemae* gen. et sp. nov.

Etymology. Ketosoma is neuter and derived from the greek words *kētos* (κῆτος), denoting a sea monster, and -soma meaning body. In Greek mythology *Keto* was a marine goddess and the sister of

Thaumas. The name refers to the relatively large body size of species in the new genus and furthermore emphasizes its strong resemblance to *Thaumastosoma*.

Distribution. Species in the genus have been described from the North and South Atlantic as well as the central and North Pacific.

Diagnosis. A1 with 6–13 articles. Mouthparts produced conspicuously forward. Md elongate, incisor process bent forward, lacinia mobilis membranous, palp well developed. Mxp with unusually long coupling hooks. Mx2 mesial endite more than half of the other endites. PI more robust than PII. Pereonite 1 somewhat larger than pereonite 2. Anterolateral margins of pereonites 1–4 with each with a robust seta. Female Op and pereonite 7 without ventral spine. Urp biramous. Sexual dimorphism modest; Plt with a pair of acute posterolateral spines in both male and female.

***Ketosoma ruehlemanni* Kaiser & Janssen gen. et sp. nov.** (Figs 9–12)
Type fixation: Holotype, ovigerous female, 5.8 mm, designated here.

Material examined. Holotype: 1 female holotype (ovigerous), 5.8 mm, CCZ, equatorial NE Pacific, BIONOD expedition, RV L'Atalante, EBS, station BIO12-33 (start: 11°49.17'N, 117°03.73'W, 4133 m; end: 11°51.91'N, 117°03.13'W, 4127 m), date: 07/04/2012, ZMH K 46133. Paratypes: 3 adult males, 1 juvenile, 1 preparatory female, from the same station as holotype, ZMH K 46134; 1 preparatory female, from the same station as holotype, ZMH K 46135; 1 preparatory female, BIONOD expedition, EBS, BIO12–43 (start: 11°45.52'N, 117°34.33', 4358 m; 11°48.34'N, 117°31.95'W, 4360 m), date: 09/04/2012, ZMH K 46136; 1 preparatory female, BIONOD expedition, EBS, BIO12–43, ZMH K 46137; 1 adult male, BIONOD expedition, EBS, BIO12–43, ZMH K 46138; 1 adult male (NBIso337), BIONOD expedition, EBS, BIO12–43, ZMH K 46139.

Etymology. The name is masculine and is dedicated to Carsten Rühlemann, one of the PIs of the BIONOD expedition.

Distribution. Eastern CCZ, equatorial NE Pacific, 4127–4360 m.

Diagnosis: A1 articles 13 in female, 11 in male; A1 article 2 with 2 broom setae distally; medial setae inserting at the distal margin of Mxp article 3; PI ischium with 7 unequally bifid ventrally; PI merus ventral margin with 2 unequally bifid setae; Op lateral and distal margins with >60 setae; Plt with one pair of posterolateral spines.

Description of holotype female. *Habitus* (Figs 9a, c, 10a, b), body length 3.9 pereonite 1 width. Coxae not visible in dorsal view. Body gradually flattening from pereonite 1 to 4 and decreasing in height from pereonites 5 to 7. Pereonites 1–7 decreasing in width; pereonite 1 widest, length 0.4 width. Pereonite 2 width 0.9 pereonite 1 width, length 0.7 pereonite 1 length. Pereonites 2 and 3 of similar length; pereonite 4 length 0.8 pereonite 1 length. Pereonites 1–4 anterior margins frontally directed, rounded, anterior lateral tergites each tipped with a small robust seta. Pereonite 5 width 0.8 pereonite 1 width. Pereonite 5 longest, length 1.2 pereonite 1 length. Pereonite 5 anterior margin slightly concave, pereonites 6–7 anterior margins convex. Plt length 0.2 body length, about as long as wide; width 0.8 pereonite 1 width, with a pair of well-developed posterolateral spines inserting 0.9 from anterior margin, posterior margin strongly rounded; anterior margin concave. Urp length 0.4 Plt length, projecting beyond posterior margin.

Cephalothorax (Figs 9a, c, 10a, b). Free, almost as long as wide. Anterior margin straight, posterior and lateral margins slightly rounded. Clypeus and labrum clearly visible from dorsal view, transition of frons, clypeus, and labrum smooth, without transverse ridge; clypeus and labrum extending 0.2 beyond frontal margin. Antennae inserting frontolaterally in a deep fold.

A1 (Fig. 9b). Length 0.1 body length, with 13 articles. First article circular and broadest, length 1.5 width, with 2 small broom setae distally. Second article length 1.3 article 1 length, length 5.4 width, with 2 long broom setae and 3 simple setae of varying length distally. Article 3 as long as article 1, length 6.0 width, with 1 simple seta distally. Article 4 length 0.2 article 1 length, length 1.8 width, with 2 simple setae distally. Articles 5–10 of similar length, length about 0.4 article 1 length, article 6 with 1 simple seta laterally. Articles 11–13 slightly shorter than articles 5–10; article 13 shortest, length 0.2 article 1 length. Article 12 with 2 simple setae of varying length distally. Article 13 with 2 long simple setae terminally.

Md (Fig. 9f, g). Md palp of left and right mandible well developed, consisting of 3 articles reaching mid of incisor. Palpal article 1 of lMd length 0.9 article 2 length, with 6 simple setae of varying length laterally. Article 2 with 2 simple setae medially. Terminal article length about one-third article 2 length, tapering distally, with several (≥ 9) small setae ventrally. Palpus of rMd similar to lMd. Incisor process of rMd lacking distinct teeth, incisor of lMd with 3 teeth and 1 subdistal tooth. Lacinia mobilis of lMd with 4 teeth. Setal row of rMd with 5 robust setae of varying size and several slender setae in between; dentation decreasing proximally. Setal row of lMd with 5 robust setae and several slender setae in between, dentation decreasing, seta size increasing proximally. Molar of rMd and lMd triangular; molar of rMd with 7, of lMd with 6 long, serrate setae distally.

Mx1 (Fig. 9d). Inner endite lost during dissection. Outer endite length 5.4 width, with 12 strong spine-like setae and 4 simple setae distally, with several simple setae of varying length laterally.

Mx2 (Fig. 9e). Outer margin of mesial endite with several setae of varying length, distal margin with numerous long setae of varying length. Mesial endite almost as long as lateral endite. Lateral endite with 4, middle endite with 3 strong setae distally.

Mxp (Fig. 9h). Left and right Mxp connected by 2 long retinacula. Epipodite smooth, triangular, slender, length 3 width, reaching mid of palpal article 2. Palpal article 1 short, width 2.6 length, with several small setae lateral. Article 2 length 2.9 article 1 length, width 1.1 length, with several small setae laterally, with 1 simple seta distally. Article 3 length 1.6 article 1 length, width 1.5 length, with 7 robust sensory setae and 1 somewhat longer simple seta distally. Article 4 length 1.5 article 1 length, width 0.4 length, with a distal projection exceeding tip of article 5, with 3 long, slender setae distally. Article 5 length 0.6 article 1 length, width 0.3 length, with 4 slender setae of varying size terminally. Endite distal margin with some robust, dentate setae and several fine setae laterally. Protopod quadrangular, length 0.9 width.

PI (Fig. 10h). More robust than PII. Basis length 2.8 width, with 8 simple setae dorsally and 3 simple setae ventrally. Ischium about half basis length, length 1.4 width, with 3 simple setae distodorsally, 1 simple seta medially (located underneath), with 7 unequally bifid and 3 simple setae ventrally. Merus length 0.6 ischium length, length 0.8 width, with 2 robust setae (1 long, 1 short) and 1 simple seta distodorsally, with 4 simple setae medially, with 2 unequally bifid and 5 simple setae of varying size ventrally. Carpus length 1.4 merus length, length 1.8 width, with a row of 12 simple setae dorsally, with 9 unequally bifid setae and 1 simple seta ventrally. Propodus length 0.9 carpus length, length 3 width, with 9 simple setae dorsally, with numerous small setae, membranously embedded, and 2 robust unequally bifid setae in between ventrally, with 2 small simple setae distoventrally. Dactylus length about half propodus length, length 3.4 width, with 3 slender setae medially. Unguis length 0.4 dactylus length, with 2 long, slender setae between unguis and ventral claw.

PII (Fig. 10i). Basis length 4.1 width, with 9 simple setae of varying length and 1 broom seta dorsally, with 1 simple seta distodorsally, with 8 simple setae ventrally and 1 long simple seta distoventrally. Ischium length about half basis length, length 2.2 width, with 5 simple setae dorsally, with 4 simple setae of varying length distodorsally, with 4 simple setae ventrally. Merus length 0.6 ischium length, length 1.2 width, with 2 simple setae of varying length distodorsally, with 5 simple setae (1 underneath) of varying size and 1 unequally bifid seta ventrally. Carpus length 2.7 merus length, length 3.5 width, with a row of 4 simple setae increasing in size medially, with 6 long slender simple setae and 8 unequally bifid setae ventrally. Propodus length 0.8 carpus length, length 5.6 width, with 2 simple setae (broken off) and 2 broom setae (1 broken off) ventrally, with numerous small

setae, membranously embedded, 6 stout unequally bifid setae (decreasing in size towards distal end) ventrally. Dactylus length one-third of propodus length, length 4.4 width, with 3 simple setae medially, with numerous small setae, membranously embedded ventrally. Unguis length 0.4 dactylus length, with 2 slender setae between unguis and ventral claw.

PIII (Fig. 10j). Basis missing. Ischium length 3.1 width, with 3 small simple setae and 1 long more robust simple seta dorsally, with 2 simple setae of varying length ventrally. Merus length 0.5 ischium length, length 1.5 width, with 1 small seta dorsally, with 2 simple setae (broken off) distodorsally, with 2 simple setae (1 broken off) ventrally, with 3 setae (1 long, 2 short) distoventrally. Carpus length 3 merus length, length 4.6 width, with 2 short simple setae dorsally, with 6 long slender setae (1 broken off) ventrally, with 8 stout unequally bifid setae ventrally. Propodus length 0.9 carpus length, length 7.7 width, with 1 broom seta distodorsally, with numerous small setae, membranously embedded, and 6 stout unequally bifid setae ventrally, with 1 simple seta distoventrally. Dactylus length 0.3 propodus length, length 4.4 width, with 3 simple setae medially. Unguis length 0.4 dactylus length, with 2 slender setae between unguis and ventral claw.

PIV (Fig. 10k). Basis length 5.7 width, with 7 simple setae and 3 broom setae (2 long, 1 short) dorsally, with 6 simple setae ventrally and 1 long simple seta distally. Ischium length half basis length, length 3 width, with 3 small simple setae dorsally, with 3 simple setae of varying size ventrally. Merus length half ischium length, length 1.7 width, with 1 long simple seta distodorsally, with 2 long simple setae distoventrally. Carpus length 3 merus length, length 5.5 width, with 2 simple setae (1 broken off) dorsally, with 5 long slender simple setae and 8 stout unequally bifid setae (1 broken off) ventrally. Propodus length 0.9 carpus length, length 8.3 width, with 8 simple setae of varying size and 1 long broom seta dorsally, with 6 stout unequally bifid setae and 1 simple seta ventrally. Dactylus length 0.2 propodus length, length 3.2 width, with 4 simple setae medially. Unguis length 0.3 dactylus length, with 2 slender setae underneath unguis.

PVI (Fig. 10l). Basis length 3.9 width, with 2 simple setae (broken off) dorsally, with 2 simple setae (1 broken off) distodorsally. Ischium length 0.6 basis length, length 2.9 width, with 4 simple setae (broken off) dorsally. Merus length 0.3 ischium length, length 1.3 width, with 2 simple setae distodorsally. Carpus length 4.6 merus length, length 3.8 width, with 4 slender setae (2 simple, 1 serrate, 1 broken off) dorsally, with 2 stout unequally bifid setae and 1 simple seta distoventrally. Propodus length 0.8 carpus length, length 6.2 width, with 10 setae (5 underneath, 2 serrate, 1 broken off) dorsally, with 7 setae (1 serrate, 1 broken off) of varying size ventrally. Dactylus length 0.3 propodus length, length 5.3 width, with 3 simple setae medially. Unguis length 0.3 dactylus length, with 2 slender setae underneath unguis.

PVII (Fig. 10m). Basis length 4.4 width, with 3 simple setae and 1 broom seta (broken off) dorsally, with 6 simple setae ventrally and 1 long simple seta distally. Ischium length 0.6 basis length, length 3.6 width, with 4 simple setae (2 broken off) dorsally. Merus length 0.3 ischium length, length 1.3 width, with 2 simple setae (broken off) distodorsally, with 2 simple setae distoventrally. Carpus length 4.2 merus length, length 4.2 width, with 8 long slender simple setae dorsally, with 4 setae (1 broken off, 1 unequally bifid) ventrally. Propodus length 0.9 carpus length, length 7.3 width, with 7 long simple setae and 1 long broom seta dorsally, with 4 stout unequally bifid setae and 1 simple seta ventrally. Dactylus length one-third of propodus length, length 6.3 width, with 3 simple setae medially. Unguis length 0.4 dactylus length, with 2 slender setae underneath unguis.

Op (Fig. 10c). Length 1.1 width. Lateral margin rounded, posterior margin almost straight, with numerous (> 60) simple setae.

Plp3 (Fig. 10d). Protopodite length 0.9 width, length 0.9 endopodite length. Exopodite 0.6 endopodite length, length 1.9 width, tapering in width distally, with numerous short simple setae laterally. Endopodite 1.2 longer than wide, with 3 long plumose setae distally, distal end tapering in an acute angle.

Plp4 (Fig. 10e). Protopodite rectangular, length 0.5 width, about 0.3 endopodite length. Exopodite slender, about as long as endopodite, length 5.8 width, with several thin setules laterally (outer margin) and 1 long robust plumose seta distally. Endopodite ovoid-shaped, length 1.5 width.

Plp5 (Fig. 10f). Small oval lobe, without setation, about as long as pleopod 4. Length 1.8 proximal width, width tapering towards distal end.

Urp (Fig. 10g). Biramous. Protopodite trapezoid, length about twice width, with 2 long simple setae laterally, with 1 small simple seta proximally, with 6 long simple setae distally. Exopodite length 1.2 protopodite length, length 7.6 width, with 5 long simple setae terminally. Endopodite length 1.5 exopodite length, length 8.6 width, with 2 simple setae (broken off) laterally, with 5 simple setae (3 broken off) terminally.

Description paratype male. *Habitus* (Figs 11a, d–e, 12a–c, e). Body length 4.8 pereonite 1 width. Coxae not visible in dorsal view. Body gradually flattening from pereonite 1 to 4 and slightly increasing in height from pereonite 5 to pleotelson. Pereonites 1–4 decreasing in width. Pereonite 1 widest, length half width. Pereonite 2 width 0.9 pereonite 1 width, length 0.6 pereonite 1 length. Pereonites 2–4 of similar length. Pereonites 1–4 anterior margins frontally directed, rounded, anterior lateral tergites each tipped with a small robust seta. Pereonites 5–7 of similar width, width 0.9 pereonite 1 width. Pereonite 5 longest, length 1.4 pereonite 1 length. Pereonite 5 anterior margin concave, pereonites 6–7 anterior margins straight. Plt 0.2 body length, about as long as wide; width 0.9 pereonite 1 width, with a pair of well-developed posterolateral spines inserting 0.8 from anterior margin, posterior margin strongly rounded, anterior margin slightly convex. Anus (Fig. 12e) covered by anus valves laterally. Urp inserting closely to the anus valves, length 0.3 Plt length, projecting beyond posterior margin.

Cephalothorax (Figs 11a, e, 12f). Free, length 0.7 width. Anterior margin straight, posterior and lateral margins slightly rounded. Clypeus and labrum clearly visible from dorsal view, transition of frons, clypeus, and labrum smooth, without transverse ridge; clypeus and labrum extending about one-third beyond frontal margin. Antennae inserting frontolaterally in a deep fold.

A1 (Figs 11a, 12a, b), from CLSM. Length 0.2 body length, with 11 articles. First article circular and broadest, length 1.7 width. Second article as long as article 1, length 6 width, with 2 long broom setae distally. Article 3 about as long as article 1, length 6.0 width. Article 4 length 0.2 article 1 length, as long as wide. Article 5 length 0.7 article 1 length, length 4 article 4 length. Articles 6–10 of similar length, length about 0.3 article 1 length. Article 11 slightly shorter than articles 6–10, length 0.2 article 1 length.

A2 (Figs 11e, 12c), from CLSM. Length 0.9 body length, with 6 peduncular and 45 flagellar articles. Peduncular articles 1–4 short. Articles 5–6 long and slender. Article 5 length 1.6 article 1–4 length, length 5 width. Article 6 length twice articles 1–4 length, length 6.1 width. Flagellar articles 1–20 swollen. Flagellar article 1 length 0.25 peduncular article 6 length. Flagellar articles 21–45 of similar length, length 0.25 article 1 length.

Plp1 (Figs 11c–d, 12e). Length 1.9 proximal width. Distal projection width 0.8 proximal width, lateral margins concave. Lateral lobes rounded, with 5 small setae inserting distally from each lateral lobe. Distal margins strongly rounded, with 6 simple setae of varying length each.

Plp2 (Fig. 11b). Sympod length 2.1 width, outer margin rounded, with 7 slender simple setae laterally, inner margin straight. Endopod inserting 0.3 from distal tip of sympod. Stylet length half sympod length, slightly curved, distal end not extending beyond distal tip of sympod. Exopod short and rounded, inserting 0.2 from distal tip of sympod.

Remarks. *K. ruehlemanni* sp. nov. shares some similarities with *K. jebamoni*, but can be delimited from the latter species by the following characters: Op with > 60 setae on lateral and distal margins (vs. ≤ 30 setae in *K. jebamoni*); A1 with 13 articles in female (vs. 11 articles); PI ischium ventral margin with 7 unequally bifid setae (vs. 4). *K. ruehlemanni* also resembles *K. distinctum*, but can be differentiated as follows: A1 with 13 articles (vs. 6 in *K. distinctum*); medial setae inserting at the distal margin of Mxp article 3 (vs. medial setae located in an arc on the ventral surface of the segment). Further details are given after the description of three new species below.

***Ketosoma hessleri* Kaiser & Brix gen. et sp. nov.** (Figs 13–14, 17a–c)

Type fixation: Holotype female, ovigerous, 4.1 mm, designated here

Material examined. Holotype: 1 female holotype (ovigerous), 4.1 mm, Vema-TRANSIT expedition (S0237), RV Sonne, C-EBS, station # 6-7 (start: 10.351389'N, 36.950278'W, end: 10.36528'N, 36.932778'W, 5085–5079), date: 02/01/2015, voucher no. VTDesm569, ZMH K 46141.

Type locality: Cape Verde Basin, eastern Vema Fracture Zone, 5085–5079 m; only known from type locality.

Etymology. The new species (*hessleri*, lat. genitive, masculine) is named in honour of Robert R. Hessler for his life dedicated to the study of deep-sea biodiversity and systematics of isopod crustaceans in particular.

Diagnosis. A1 articles 13 in female; A1 article 2 with 3 broom setae distally; medial setae inserting at the distal margin of Mxp article 3; PI ischium with a row of simple setae on ventral margin; PI merus ventral margin with 4 unequally bifid setae; Op lateral and distal margins with >50 setae; Plt with one pair of posterolateral spines.

Description of holotype female. *Habitus* (Figs 13a, c, 14f, 17a–c), body length 3.5 pereonite 1 width. Coxae not visible in dorsal view. Pereonites 1–7 decreasing in width. Pereonite 1 widest, length 0.3 width. Pereonite 2 width 0.9 pereonite 1 width, length 0.8 pereonite 1 length (measured from lateral view). Pereonites 2 to 4 of similar length (measured laterally). Pereonites 1–4 anterior margins frontally directed, rounded, anterior lateral tergites each tipped with a small robust seta. Pereonite 5 width 0.9 pereonite 1 width. Pereonite 5 longest, length 1.6 pereonite 1 length (measured laterally). Pereonite 5–7 anterior margins slightly concave. Plt length 0.2 body length, about as long as wide (measured laterally), width 0.8 pereonite 1 width, with a pair of well-developed posterolateral spines inserting 0.9 from anterior margin, posterior margin strongly rounded, anterior margin concave. Urp length 0.4 Plt length, projecting beyond posterior margin.

Cephalothorax (Figs 13a–d, 14 f, 17a–b). Free, length almost as long as wide (measured laterally). Anterior margin straight, posterior and lateral margins slightly rounded. Transition of frons, clypeus, and labrum smooth, without transverse ridge (Fig. 17b). Antennae inserting frontolaterally in a deep fold.

A1 (Fig. 13b). Length 0.25 body length, with 13 articles. First article circular and broadest, length 1.8 width. Second article length 1.2 article 1 length, length 6.5 width, with 3 broom setae distally. Article 3 length 0.6 article 1 length, length 4.7 width. Article 4 length 0.2 article 1 length, length 1.3 width. Articles 5–13 of similar length, length 0.4 article 1 length.

LMd (Fig. 14a), palpus broken off. Incisor process with 3 teeth and 1 subdistal tooth. Lacinia mobilis with 3 teeth. Setal row with 6 robust setae and 3 slender setae in between, dentation decreasing, seta size increasing proximally. Molar triangular, with 5 long setae distally.

Mx2 (Fig. 14b) Outer margins of mesial endite with several setae of varying length. Mesial slightly longer than lateral and middle endites. Lateral and middle endite each with 4 strong setae distally.

Mxp (Fig. 14c–d), only palpal articles 2–5 and endite drawn *in situ*. Left and right Mxp connected by 3 long retinacula. Palpal article 2 almost as long as wide; with several small setae laterally, with 4 simple setae distally. Article 3 length 0.9 article 2 length, width 0.8 length, with 11 robust sensory setae located in an arc on the ventral surface of the segment. Article 4 length 0.6 article 2 length, width 0.3 length, with a distal projection exceeding tip of article 5, with 4 long, slender setae distally. Article 5 length 0.2 article 2 length, width 0.3 length, with 4 slender setae of varying size

terminally. Endite distal margin with some robust, dentate setae and several fine setae on lateral and ventral margins.

PI (Fig. 13e). Drawn *in situ*. Basis not drawn. Ischium length 1.3 width, with 12 simple setae of varying size dorsally, with 6 simple setae ventrally. Merus length 0.6 ischium length, length 0.7 width, with a row of 9 simple setae (1 broken off), extending from medial surface to distodorsal end, with 2 robust unequally bifid setae (1 long, 1 short) distodorsally, with 3 simple setae and 4 robust unequally bifid setae ventrally increasing in size distally. Carpus length 1.6 merus length, length 1.2 width, with 11 simple setae of varying size dorsally, with 8 unequally bifid setae ventrally increasing in size distally. Propodus as long as carpus, length 2.9 width, with 3 simple setae dorsally, with numerous small setae, membranously embedded, and 2 robust unequally bifid setae in between ventrally. Dactylus length 0.6 propodus length, length 4 width, with 3 slender setae medially. Unguis length 0.5 dactylus length, with 2 long, slender setae underneath unguis.

PVI (Fig. 14e). Basis length 4.9 width, with 5 simple setae and 5 broom setae dorsally, with 5 simple setae dorsally, with 1 long simple seta distodorsally. Ischium length half basis length, length 3.1 width, with 6 simple setae dorsally, with 4 simple setae ventrally. Merus length 0.3 ischium length, length 1.5 width, with 2 simple setae distodorsally, with 1 simple seta ventrally. Carpus length 3.9 merus length, length 4.1 width, with 6 setae (all broken off) dorsally, with 5 simple setae ventrally. Propodus length 0.8 carpus length, length 6.7 width, with 7 long serrate setae (1 broken off) and 1 unequally bifid seta dorsally (see detail), with 4 stout unequally bifid setae ventrally. Dactylus length 0.4 propodus length, length 7.4 width, with 3 simple setae medially, with numerous small setae, membranously embedded, ventrally. Unguis length 0.4 dactylus length, with 2 slender setae underneath unguis.

Op (Fig. 17c), from CLSM. Length 1.1 width. Lateral margin rounded, posterior margin slightly concave, with numerous (> 50) simple setae.

Remarks. *K. hessleri* sp. nov. is most similar to *K. ruehlemanni* and *K. jebamoni.* All three species differ from *K. distinctum* in the number of antennular articles (≥11 vs. 6). *K. hessleri* can be further distinguished from *K. ruehlemanni* by the following characters: PI ischium with a row of simple setae on ventral margin (vs. unequally bifid in *K. ruehlemanni*); A1 article 2 with 3 broom setae (vs. 2); medial setae located in an arc on the ventral surface of the segment of Mxp article 3 (vs. medial setae inserting at the distal margin). The new species also shows some resemblance to *K. jebamoni*, but differs from the latter as follows: A1 with 13 articles in female (vs. 11 articles in *K. jebamoni*); PI merus ventral margin with 4 unequally bifid setae (vs. 7).

***Ketosoma vemae* Brix & Kihara gen. et sp. nov.** (Figs 15–17d–f)
Type fixation: Holotype adult male, 3.7 mm, designated here.

Material examined. Holotype: 1 male holotype (adult), 3.7 mm, equatorial NE Atlantic, Vema-TRANSIT expedition (SO237), RV Sonne, C-EBS, station # 2-6 (start: 10.709167'N, 25.0994'W, end: 10.72667`N, 25.086667'W, depth: 5520 m), date: 20/12/2014, voucher No. VTDesm013, ZMH K 46140.

Type locality: Cape Verde Basin, eastern Vema Fracture Zone, 5520 m; only known from the type locality.

Etymology. The name is genitive female and relates to the sampling campaign (Vema-TRANSIT) as well as the type locality, where the type specimen was collected.

Diagnosis. A1 articles 11 in male; A1 article 2 with 4 broom setae distally; medial setae located in an arc on the ventral surface of the segment of Mxp article 3; PI ischium with 4 unequally bifid setae

ventrally; PI merus ventral margin with 2 unequally bifid setae; Plt with one pair of posterolateral spines.

Description of holotype male. *Habitus* (Figs 15a, d, 17d–e), body length 4.9 pereonite 1 width. Coxae not visible in dorsal view. Body gradually flattening from pereonite 1 to 6 and increasing in height from pereonite 6 to Plt. Pereonites 1–4 decreasing in width. Pereonite 1 widest, length 0.6 width. Pereonite 2 width 0.9 pereonite 1 width, Pereonite 2 and 3 similar in length; length about half pereonite 1 length. Pereonite 3 and 4 similar in width. Pereonite 3 width 0.8 pereonite 1 width. Pereonite 4 length 0.6 pereonite 1 length. Pereonites anterior margins 1–4 frontally directed, rounded, anterior lateral tergites each tipped with a small robust seta. Pereonites 5–7 decreasing in width distally. Pereonites 5 width 0.8 pereonite 1 width. Pereonite 5 longest, length 1.4 pereonite 1 length. Pereonite 5 anterior margin slightly concave, pereonites 6–7 anterior margins straight. Plt length 0.2 body length, about as long as wide, width 0.8 pereonite 1 width, with a pair of well-developed posterolateral spines inserting 0.8 from anterior margin, posterior margin strongly rounded. Urp length 0.4 Plt length, projecting beyond posterior margin.

Cephalothorax (Figs 15a–d, 17d–f). Free, length 0.7 width. Anterior margin strongly rounded, posterior and lateral margins straight. Transition of frons, clypeus, and labrum smooth, without transverse ridge (Fig. 17f). Antennae inserting frontolaterally in a deep fold.

A1 (Fig. 16a). Length 0.3 body length, with 11 articles. First article rectangular, broadest, length 1.5 width, with 2 broom setae distally. Second article length 1.5 article 1 length, length 3.8 width, with 4 long broom setae distally. Article 3 length 1.1 article 1 length, length 4.3 width, with 1 simple seta distally. Article 4 shortest, length 0.3 article 1 length, length 1.2 width, with 1 simple seta and 1 small broom seta distally. Articles 5–10 of similar width. Article 5 length 0.9 article 1 length, length 4.5 width, with 1 small simple seta distally. Article 6 length 0.6 times article 1 length, length 3 width, with 1 small simple seta distally. Articles 7–10 of similar length, length 0.7 article 1 length, length 4.3 width. Article 7 and 9 each with 1 small simple seta distally. Article 10 with 1 long aesthetasc. Article 11 with 1 small broom seta, and 4 simple setae (2 broken off) terminally.

Mxp (Fig. 16c). Only the palpus drawn *in situ*. Palpal article 1 short, width 2.3 length, with several small setae and 1 long slender seta laterally. Article 2 length 3 article 1 length, almost as wide as long, with several small setae proximally, with 8 distally pappose sensillae, 1 dentate seta, two rows of small setule and 1 simple setae distolaterally. Article 3 length twice article 1 length, width 1.2 length, with 7 distally pappose sensillae arranged in an arc on the Mxp ventral surface, with 1 slender and 2 small simple setae laterally. Article 4 length 1.8 article 1 length, width 0.3 length, with a distal projection exceeding tip of article 5, with 3 long distally pappose sensillae distally, with numerous small simple setae laterally. Article 5 length half article 1 length, width half length, with 4 slender setae of varying size terminally.

PI (Fig. 16g–h). Drawn in *situ*, left PI illustrated basis to merus, right PI merus to dactylus. Basis length 2.9 times width, with 3 simple setae and 1 small broom seta dorsally, with 4 simple setae (1 broken off) ventrally. Ischium length 0.6 basis length, length 1.9 times width, with 1 slender seta (broken off) and 1 robust seta dorsally, with 4 unequally bifid setae and 1 simple seta ventrally. Merus length 0.4 times ischium length, length 0.7 width, with 2 robust unequally bifid setae (broken off in left PI) distodorsally, with 4 simple setae medially, with 2 unequally bifid and 2 robust setae (broken off in left PI) distoventrally. Carpus length 1.5 times merus length, length 1.3 times width, with 1 simple seta distodorsally, with 7 unequally bifid setae ventrally. Propodus length 1.2 times carpus length, length 4.1 times width, with 3 simple setae and 1 small broom seta dorsally, with numerous small setae, membranously embedded, 1 robust unequally bifid seta and 1 simple seta in between ventrally. Dactylus length about half propodus length, length 3.6 times width, with 3 slender setae medially. Unguis length 0.3 times dactylus length, with 2 long, slender setae between unguis and ventral claw.

PIII (Fig. 16d). Basis missing. Ischium length 3.3 width, with 3 simple setae (1 broken off) dorsally, with 3 simple setae (1 broken off) ventrally. Merus length 0.6 ischium length, length 1.7

times width, with 1 long robust seta distodorsally, with 3 simple setae of varying size ventrally. Carpus length 3.2 merus length, length 4.7 width, with 12 setae (5 broken off) dorsally, with 4 long slender setae, numerous small setae, membranously embedded, and 7 stout unequally bifid setae in between ventrally. Propodus length 0.9 carpus length, length 4.6 width, with 3 simple setae of varying size (1 broken off) and 1 broom seta dorsally, with numerous small setae, membranously embedded, and 5 stout unequally bifid setae in between ventrally. Dactylus length 0.4 propodus length, length 4.6 width. Unguis length 0.4 dactylus length, with 2 slender setae underneath unguis.

PIV (Fig. 16e). Basis length 6.2 width, with 1 long broom seta and 1 simple seta dorsally, with 5 broom setae and 1 short simple seta ventrally. Ischium length 0.6 basis length, length 3.8 width, with 2 short simple setae dorsally, with 2 short simple setae ventrally. Merus length 0.4 ischium length, length 1.7 width, with each 1 simple seta distodorsally and distoventrally. Carpus length 3.5 merus length, length 5.8 width, with 1 simple seta (broken off) distodorsally, with numerous small setae, membranously embedded and with 7 setae (3 unequally bifid, 1 simple, 3 broken off) in between ventrally. Propodus length 0.9 carpus length, length 7.4 width, with 4 setae (all broken off) and 1 broom seta dorsally, with numerous small setae, membranously embedded and with 5 setae (1 unequally bifid and 4 broken off) ventrally. Dactylus length 0.3 propodus length, length 4.5 width, with 3 simple setae medially. Unguis length 0.4 dactylus length, with 2 slender setae underneath unguis.

PV (Fig.16f). Basis length 4.1 width, with 6 simple setae dorsally, with 2 simple setae and 1 broom seta dorsally. Ischium length 0.6 basis length, length 2.7 width, with 1 simple seta dorsally, with 5 slender simple setae of varying size ventrally. Merus length 0.4 ischium length, length 1.5 width, with 2 simple setae distodorsally. Carpus length 3.7 merus length, length 2.8 width, with 10 slender setae (6 long simple, 1 short simple, 2 long serrate, 1 broken off) dorsally, with 7 setae (4 unequally bifid, 3 broken off) ventrally. Propodus length 0.9 carpus length, length 4.6 width, with 8 simple setae of varying size dorsally, with 7 long slender setae (all tips broken off) ventrally. Dactylus length 0.3 propodus length, length 5 width, with 3 simple setae medially. Unguis length about half dactylus length, with 2 slender setae underneath unguis.

Remarks. *Ketosoma vemae* sp. nov. can be easiliy distinguished from *K. distinctum* by the number of A1 articles (11 vs. 6). As for *K. vemae* only the male is known, it is difficult to define characters distinguishing it from *K. hessleri* and *K. jebamoni*, where only female specimens have been collected. The new species, for example, resembles *K. jebamoni* in the number of antennula articles, though it also shows some distinct features separating it from the latter: PI merus with 2 long unequally bifid setae distodorsally (vs. 1 simple seta in *K. jebamoni*); PI merus ventral margin with 2 unequally bifid setae (vs. 7); A1 article 1 with 2 broom setae (vs. none). The new species is also similar *to K. ruehlemanni*, but can be distinguished as follows: medial setae located in an arc on the ventral surface of the segment of Mxp article 3 (vs. medial setae inserting at the distal margin in *K. ruehlemanni*). *K.* vemae can be differentiated from *K. hessleri* by the following characters*:* A1 article 2 with 4 broom setae distally (vs. 3 in *K. hessleri*); PI ischium with 4 unequally bifid setae (vs. only simple setae present); PI merus ventral margin with 2 unequally bifid setae (vs. 4).

***Ketosoma werneri* Kaiser & Brix gen. et sp. nov.** (Figs 18–19)
Type fixation: Holotype female, preparatory, 2.1 mm (measured without Plt), designated here.

Material examined: Material examined. Holotype: 1 female holotype (preparatory), 2.1 mm, Argentine Basin, SW Atlantic, DIVA-3 expedition (M79), RV Meteor, EBS, station # 534 (start: 36.01016'S, 49.02566'W, end: 36.0115'S, 49.029'W, depth: 4608 m), date: 16/07/2009, voucher no. D3D060, ZMH K 46142.

Type locality: Argentine Basin, SW Atlantic, 4608 m; only known from type locality.

Etymology. The name is genitive masculine and dedicated to Werner Rosenboom, participant of the DIVA-2 expedition, and Werner Harke, uncle of the first author, passing away in 2006 and 2009 respectively.

Diagnosis. A1 with 6 articles; pereonite 7 length ≤0.4 pereonite 6 length; PI ischium with 2 unequally bifid setae on ventral margin; Op lateral and distal margins with 10 setae; Plt posterior margin smooth, with one pair of posterolateral spines.

Description of holotype female. *Habitus* (Figs 18a, c–d, 19a–b), body length 4.4 pereonite 1 width. Coxae of pereonite 2 visible in dorsal view. Body gradually flattening from pereonite 1 to 6 and increasing in height from pereonite 6 to Plt. Pereonites 1–4 decreasing in width, pereonites 4–7 of similar width. Pereonite 1 widest, length half width. Pereonite 2 width 0.9 pereonite 1 width, length 0.6 pereonite 1 length. Pereonites 2–4 of similar length. Pereonite 4 width 0.75 pereonite 1 width. Pereonites 1–4 anterior margins frontally directed, rounded, anterior lateral tergites each tipped with a small robust seta. Pereonite 5 longest, length 1.1 pereonite 1 length. Pereonite 5–7 anterior margins straight. Pereonite 6 length 0.9 pereonite 1 length. Pereonite 7 length half pereonite 1 length. Plt length 0.2 body length, length 0.9 width, width 0.8 pereonite 1 width, with a pair of well-developed posterolateral spines inserting 0.9 from anterior margin, posterior margin strongly rounded, anterior margin concave. Urp length 0.5 Plt length, projecting beyond posterior margin.

Cephalothorax (Figs 18a, d, 19b). Free, length 1.4 width. Anterior margin straight, posterior and lateral margins slightly rounded. Clypeus and labrum clearly visible from dorsal view, transition of frons, clypeus, and labrum smooth, without transverse ridge; clypeus and labrum extending 0.2 beyond frontal margin. Antennae inserting frontolaterally in a deep fold.

A1 (Fig. 18b*).* Drawn *in situ*. Length 0.2 body length, with 6 articles. First article rectangular, broadest, length 1.3 width, with 2 broom small setae and 1 simple seta distally. Second article length 1.3 article 1 length, length 3 width, with 2 long broom setae and 1 small simple seta distally. Article 3 as long as article 1, length 2.7 width, with 1 small simple seta distally. Article 4 length half article 1 length, length 1.3 width, with 2 broom setae distally. Articles 5 length 1.1 article 1 length, article 6 about as long as article 1, length 5 width, with 4 long simple setae and 1 aesthetasc terminally.

A2 (Fig. 18b*).* Drawn *in situ*. Length 0.9 body length, with 6 peduncular and 17 flagellar articles. Peduncular articles 1–4 short. Article 1 with 1 simple seta laterally Article 3 with 1 unequally bifid and 1 simple seta laterally. Article 4 with 1 simple seta laterally. Articles 5–6 long and slender. Article 5 length 1.4 article 1–4 length, length 6.5 width, with 3 robust unequally bifid setae, 3 broom setae and 2 simple setae of varying size laterally. Article 6 length 2.5 article 1–4 length, length 11.7 width, with 1 simple seta laterally, with 1 broom seta and 1 slender seta distally. Flagellar article 1 length 0.2 article 6 length. Flagellar articles 1–17 length ratios: 1 : 1 : 0.6 : 0.9 : 0.6 : 0.6 : 0.6 : 0.8 : 0.8 : 0.7 : 0.9 : 0.5 : 0.6 : 0.6 : 0.5 : 0.3 : 0.2. Articles 1–16 with 0–3 simple setae distally, article 17 with 6 long, slender setae terminally.

PI (Fig. 18f). Basis length 3 width, with 1 long robust simple seta distoventrally. Ischium 0.4 basis length, length 1.5 width, with 2 simple setae of varying size dorsally, with numerous small setae, membranously embedded, and 3 unequally bifid (1 broken off) setae ventrally. Merus length 0.6 ischium length, as long as wide, with 2 long robust unequally bifid setae distodorsally, with numerous small setae, membranously embedded, 2 slender simple setae and 2 robust unequally bifid setae (1 underneath) ventrally. Carpus length 1.7 merus length, length 1.5 width, with 3 simple setae dorsally, with numerous small setae, membranously embedded, 4 unequally bifid setae and 1 simple seta in between ventrally. Propodus as long as carpus, length 2.5 width, with 1 simple seta distodorsally, with numerous small setae, membranously embedded, 1 small unequally bifid seta and 1 simple seta in between ventrally. Dactylus 0.6 propodus length, length 3.5 width, with 3 slender setae medially. Unguis length 0.3 dactylus length, with 2 long, slender distally pappose setae between unguis and ventral claw.

PIV (Fig. 18g). Drawn *in situ*. Basis length 4.7 width, with 2 broom setae medially, with 3 simple setae ventrally. Ischium length 0.7 basis length, length 3.6 width, with 1 simple seta ventrally. Merus length 0.6 ischium length, length 1.9 width, with 2 long simple setae distodorsally, with 2 long simple setae distoventrally. Carpus length 2.6 merus length, length 6.1 width, with 3 simple setae (1 broken off) medially, with numerous small setae, membranously embedded, and 2 unequally bifid setae in between ventrally. Propodus length 0.8 carpus length, length 5.4 width, with 1 long simple seta dorsally, with numerous small setae, membranously embedded, 2 stout unequally bifid setae and 1 simple seta in between ventrally. Dactylus length 0.6 propodus length, length 5 width, with 3 simple setae medially. Unguis length half dactylus length, with 2 slender distally pappose setae underneath unguis.

PVI (Fig. 18h). Drawn *in situ*. Basis length 4.5 width, with 1 simple seta distoventrally. Ischium length 0.7 basis length, length 3.3 width, with 1 simple seta dorsally, with 1 simple seta ventrally. Merus length 0.3 ischium length, length 1.2 width, with 2 simple setae distodorsally, with 2 simple setae distoventrally. Carpus length 4.4 merus length, length 6.4 width, with 1 slender seta dorsally, with 1 simple seta and 1 broom seta distodorsally, with 2 long simple setae ventrally. Propodus length 0.8 carpus length, length 7.5 width, with 3 simple setae of varying size dorsally, with 1 simple seta distoventrally. Dactylus length about half propodus length, length 5 width. Unguis length 0.7 dactylus length, with 2 slender distally pappose setae underneath unguis.

Op (Fig. 18e). Drawn *in situ*. As long as wide. Lateral and posterior margins rounded. Lateral margin with 4 simple setae, distal margin with 6 simple setae.

Remarks. Based on the number of the antennula articles two species clusters can be differentiated within *Ketosoma*; one formed by *Ketosoma werneri* sp. nov. together with *K. distinctum* each bearing 6 antennula articles and one containing *K. ruehlemanni*, *K. hessleri*, *K. vemae* and *K. jebamoni* (A1 with ≥11 articles). *K. werneri* and *K. distinctum* share some further similarities including pereonite 7 length ≤0.4 pereonite 6 length, and number of setae on Op lateral and distal margins with ≤10 (vs. pereonite 7 length ≥0.6 pereonite 6 length; Op lateral and distal margins with ≥30 setae in the remaining species, if known). The new species can be differentiated from *K. distinctum* as follows: Plt bearing only one pair of posterolateral spines, posterior margin smooth (vs. Plt with two pairs of posterolateral spines [2 large and 2 minute] distally, Plt posterior margin with fringe of tiny setules); Op as long as wide, with 4 setae laterally (vs. Op longer than wide, lacking lateral setae); PI ischium with 2 unequally bifid setae on ventral margin (vs. PI ischium lacking ventral setae). It should be noted, that morphological characters of *K. distinctum* are inferred from illustrations by Birstein (1963). Once the type material becomes available, it should be closely re-examined to provide a more reliable comparision.

4. Discussion

4.1 Integrative species delimitation

Combining information from multiple sources to delineate species is now more commonly adopted as the foundation for subsequent biodiversity assessment. In fact, there is the proposal to perform a number of species delimitation analyses and then to define species boundaries being most consistent across methods to overcome potential limitations (Carstens et al., 2013). In our study, we provided morphological and genetic evidence to erect a new genus, *Ketosoma* that shows distinct features separating it from the closely related *Thaumastosoma*. Furthermore, species delimitation analyses of the molecular data were mostly congruent with *a priori* morphological presumptions to differentiate species within both genera. However, low sample sizes (as in number of individuals per clade) are raising some issues to both morphological and molecular species delimitation methods, as all are sensitive to undersampling (e.g. Lohse, 2009; Lim et al., 2012).

The *Ketosoma vemae/hessleri* clade highlights such a dilemma, where neither morphological nor molecular examination provided unequivocal evidence for species differentiation. Morphological

differentiation is complicated by the fact that *K. vemae* and *K. hessleri* are singleton species and holotypes are represented by the opposite sex. Thus, morphological differences may be obscured by potentially sexually dimorphic features. So far, the only characters distinguishing both species from each other are the type and number of setae on the ventral margins of PI ischium and merus, and the antennula. Most but not all SD analyses delimited *K. vemae* and *K. hessleri* as separate species (Fig. 2). The divergence between both specimens was about 5.14% uncorrected p-distance in 16S, which lies above the ABGD threshold of 1-4% calculated from the specimens herein (Table 4). A few other similar analyses on deep-sea isopods are available for additional comparison. For *Atlantoserolis vemae*, a widespread species across the Atlantic, Brandt et al. (2014) found a gap between 2.5% and 4.7% for 16S to separate between intraspecific and congeneric divergence. In the desmosomatid species *Parvochelus russus*, Brix et al. (2015) found a genetic variation of 3.8% uncorrected p-distances for 16S between specimens occuring on both sides of the Mid-Atlantic Ridge (MAR). For this species the authors suggest infrequent connectivity across the MAR (i.e., through the Romanche Fracture Zone, Brix et al., 2015). In ABGD analyses of 195 South Atlantic desmosomatid and nannoniscid specimens (comprising 15 genera), Brix et al. (this issue) detected a barcode gap of 4% at 16S; genus-specific analyses of the desmosomatids *Chelator* (61 specimens), *Mirabilicoxa* (12 specimens), and *Parvochelus* (9 specimens) detected barcode gaps beginning at 3.0%, 4.5%, and 1.5% at 16S, respectively (Brix et al., this issue). It should be noted that the seemingly different thresholds for *Parvochelus* (Brix et al., 2015 vs. Brix et al., this issue) arise from the use of different data sets (one including specimens of *Parvochelus russus* only, one comprising additional species in the genus, cf. Brix et al., this issue). Thus, defining unified thresholds across different evolutionary lineages has some limitations, in that such lineages represent a spectrum of evolutionary ages and histories, which may differ across taxa and markers (Brix et al., 2015). Nevertheless, using these estimates as additional means of comparison, *K. vemae* and *K. hessleri* would be considered as separate species.

Molecular species delimitation methods do not necessarily require (or measure) reciprocal monophyly between delimited species; rather, most invoke a multispecies coalescent model in which some aspect of the evolutionary process (patterns in evolutionary rates, branch length distributions, etc.) changes across the intra- vs. interspecific threshold. Even though, reciprocal monophyly was difficult to establish in some cases here, when the putative species were delimited from a single specimen. As De Queiroz (2007, p. 884) points out, because of the maternal inheritance of mitochondrial DNA, "a pattern of reciprocal monophyly can also result from low dispersal distances of females even when autosomal and paternally inherited genes are being exchanged regularly between the same sets of populations […]". While the sequencing success of nuclear 18S was not high, moreover its low mutation rate made it rather uninformative to delineate species in these two closely related genera. Finally, the existence of doubly uniparental inheritance (DUI, e.g. Passamonti and Ghiselli, 2009) of mitochondrial markers could complicate the interpretation, although to our knowledge no evidence of DUI has been reported for asellotes. Even though male- and female-type mitochondrial sequences are not necessarily each other's closest relatives, DUI is often detected when highly aberrant sequences are recovered from a single individual or putatively conspecific individuals, and no evidence of this was found here. Likewise no specimen produced chromatograms with evidence of divergent, overlaid sequences, nor were the coding errors typical of male mitochondrial DNA encountered. Accordingly, we regard *Ketosoma vemae* and *K. hessleri* as separate species. It is possible that both species represent recently diverged conspecific lineages becoming reproductively isolated through geographic and separation. Recently diverged species are expected to retain ancestral polymorphisms due to incomplete lineage sorting, and incipient (i.e. ongoing) speciation can generate a similar signal as reproductive isolation increases, as has been found in other marine invertebrates (e.g. Johnson et al., 2006; Baird et al., 2011; Schüller, 2011; Jennings et al. 2013).

Likewise *Ketosoma* specimens in the so far undescribed Pacific clade (containing KM14 and NB12 specimens) were not separated by all SD methods. For NB12_Iso740_9 only sequence data from 18S was available; due to the overall paucity of 18S data in the study the AGBD results remain inconclusive though. Furthermore, as a slowly evolving marker it is better suited to explore supra-

specific relationships. Here, greater taxon sampling as well as morphological examination of the Pacific clade may provide important hints to resolve within-clade patterns.

Molecular species delimitation is a nascent and quickly-evolving field; currently no single methodology is considered superior in all cases, but rather concordance is sought between multiple methods, particularly with discovery methods. While ABGD requires very few assumptions and is easily comparable across taxa, it makes only simple comparative, not phylogenetic use of the data. The bPTP and GMYC methods both employ a multispecies coalescent model; however, GMYC requires a strictly ultrametric tree, and the multiple threshold version tends to underperform the single threshold version (Fujisawa and Barraclough, 2013). Indeed, the results of ABGD, bPTP, and GMYCsingle were all consistent, and these delimitations received high validation support by BPP (≥90), suggesting that the complications of small taxon size and missing sequences did not overwhelm the signal in the data. The most parameter-rich and complex analysis is STACEY, where the species tree and its delimitations are estimated simultaneously; although the STACEY results were broadly consistent with the others, the dataset's complications probably affected STACEY moreso than other SD algorithms.

4.2 Taxonomic considerations

Besides genetic differentation between *Ketosoma* and *Thaumastosoma*, both genera are well defined by morphological means (summarized above). However, the taxonomic value of ventral spines present on pereonite 7 and operculum as a synapomorphic character in *Thaumastosoma* is not unambiguously solved. Ventral spines are also present in the related Desmosomatidae G.O. Sars, 1897 and Macrostylidae Hansen 1916. It is likely that spines evolved independently in the three families, as they are located on different pereonites and their shape varies across taxa (but see Wägele, 1989). For example, in Desmosomatidae ventral spines are limited to the pereonites 1–5 (e.g. in *Prochelator lateralis* (Sars, 1899), *Disparella kensleyi* Brix, 2006). In Macrostylidae the position of ventral spines varies across pereonites, and is regarded as an important diagnostic character to separate species within the (monogeneric) family (T. Riehl, pers. communication). Within Nannoniscidae, ventral spines on the fused pereonites 6 and 7 are reported as as a synapomorphy of species within *Regabellator* Siebenaller & Hessler, 1981. However, in the genera *Nannoniscus* G.O. Sars, 1870 and *Rapaniscus* Siebenaller & Hessler, 1981 the position and shape of ventral spines varies greatly. In a recent paper, Wilson (2008) re-evaluated the classification of the genera in Nannoniscidae with special emphasis on *Nannoniscus*. Wilson (2008) discussed the variable position of the ventral spines within the genus, yet did not accord this character great diagnostic value. *Nannoniscus teres* Siebenaller & Hessler, 1981 possesses a caudally directed strong spine on pereonite 7, *N. analis* Hansen, 1916 has a caudally directed curved spine on the operculum and *N. bidens* (*sensu* Brandt, 1992, cf. Wilson, 2008) and *N. antennaspinis* Brandt, 2002 have a straight, but caudally directed spine on their opercula, while some species do not possess any ventral spine (e.g., *N. aequiremus* Hansen, 1916). In *Thaumastosoma*, a small straight spine on pereonite 7 and a strong midventral spine on the operculum are present, which seems to be consístent in two *Thaumastosoma* species, but cannot be seen in *T. diva* due to damage of the holotype.

Additionally, there has been some debate whether posterolateral spines are present in *Thaumastosoma* or not (Hessler, 1970; George, 2001; Wilson, 2008). We argue, in the line with Wilson (2008), that both genera possess posterolateral spines, yet, where known, the shape differs (acute in *Ketosoma* vs. broad in *Thaumastosoma*) as well as the degree of differentiation between male and female (hardly any difference in *Ketosoma* vs. highly sexually dimorphic in *Thaumastosoma*).

Sexual dimorphism seems to be only weakly developed in *Ketosoma*, while still being an issue as male and female are only known from one species. We discussed this problem in more detail with reference to the differentiation of *Ketosoma vemae* and *K. hessleri* above. Due to paucity of data it is not possible to draw final conclusions as to which characters are conservative between male and female and thus informative to separate species (cf. Riehl et al., 2012). In this respect, it is not clear whether the difference in the number of antennula articles between male and female is gender-related

(11 in male vs. 13 in female), and furthermore if this is consistent across all *Ketosoma* species. For example, in the female holotype of *K. jebamoni* only 11 articles were illustrated (George, 2001). This is further complicated by the fact that some *Ketosoma* species possess ≥ 11 antennula articles, a number quite unusual among nannoniscids, compared to only six in *Ketosoma distinctum* and *K. werneri.* The latter two species bear additional characters, which clearly assign them to *Ketosoma*, but at the same time show features separating them from the remaining species in the genus (e.g. including setation operculum distal margin and size of pereonite 7). Genetic data are only available from *K. werneri*, which, in our study, has been assigned to a well-supported Atlantic clade within the new genus (Figure 1). However, with future sampling more specimens and species in the *Ketosoma* clade may become available, which could be used to fine-tune phylogenetic patterns.

4.3 Implications for deep-sea biodiversity and biogeography

Most species descriptions herein are based on individual specimens. One could argue that when describing singleton species means that intraspecific variability cannot be assessed (cf. Dayrat 2005). However, rarity represents a common feature of the deep-sea fauna (e.g. Brandt et al., 2007; Janssen et al., 2015), and thus a large fraction of its diversity would remain undescribed (Lim et al., 2012).

Overall geographic patterns and mechanisms of species' distributions are still poorly understood leading to some contraints on assessing broad-scale diversity patterns (Appeltans et al., 2012). Due to their predominant reproductive mode (as being brooders) restricted ranges in isopods, as seen in our study, would not be surprising (see also Raupach et al., 2007; Brix et al., 2011; Janssen et al., 2015; Brix et al., this issue; Riehl et al., this issue). On the contrary though, there is also evidence for some isopod species to maintain gene flow across relatively large geographic distances (hundreds to thousands of kms; e.g. Riehl and Kaiser, 2012; Janssen et al., 2015; Brix et al., 2015, this issue, Riehl et al., this issue). Based on our analyses, species within each genus seem to have a very narrow distributional range. Furthermore, in the CCZ we found several *Ketosoma* species to occur at relatively small spatial scales (few km to tens of kms apart, Table 2; see also Janssen et al., 2015). In fact, *Thaumastosoma platycarpus* seems to be the only species with a broader distribution (specimens collected >4000 km apart, Fig. 1, Tables 2, 7), but material of *T. platycarpus* from the Iceland Basin examined here (Table 2) could not be assigned to this species with final certainty due to damage of the specimens.

Along the Vema Fracture Zone species most isopod lineages within the families Desmosomatidae, Nannoniscidae (including *K. vemae* and *K. hessleri*) and Macrostylidae showed limited geographic distributions either restricted to one station and/or one side of the MAR, and only few species were found at both sides of the MAR (Brix et al., 2015, this issue, Riehl et al., this issue). This is in support of the hypothesis that the MAR in fact presents a dispersal barrier, at least for isopods, but also geographic distance itself and prevailing hydrographic conditions have been identified as important factors to shape faunal distributions in the abyss amongst others (Janssen et al., 2015; Brix et al., this issue; Guggolz et al., this issue; Riehl et al., this issue; but see Etter et al., 2005)

Although data presented here are rather limited, they cover some general issues reported for deep-sea samples (e.g. with regard to sexual dimorphism, rarity, and undersampling). So it is very likely that with further sampling singleton species will occur at more sites, but at the same time the number of rare species will increase (as seen for other environments, Lim et al. 2012). The way forward is to account for rarity and low sample sizes by using multiple lines of evidence to maximize the accuracy of species delimitations. However, it is interesting to note that, in our case, SD delimitations tend to vary in the same situations where morphological data are likewise not straightforward - implying that the most interesting (biological) questions are the most difficult to answer definitively.

Acknowledgements

The authors would like to thank the masters, crew and participants of RV Sonne, RV L'Atalante, RV Kilo Moana and RV Meteor. Special thanks are due to Courtney Wickel, Chad Walters, Karen Osborn (USNM), Kirill Minin (Shirshov Institute of Oceanology, Russian Academy of Science, Moscow), Stephen Keable (Australian Museum, Sydney) and Bob George for their help tracking the type material of *Thaumastosoma* s.l. species. Karen Jeskulke is thanked for her help with the lab work. Amy Driskell helped with the data processing at the Smithsonian and uploading all information to BOLD. Antje Fischer and Sven Hoffmann (DZMB) are thanked for helping with the scans and allocation of the type material. Thanks are also due to Kai George for valuable discussions in the early stage of the study. Furthermore, the authors acknowledge valuable comments received by two anonymous reviewers. The BIONOD expedition was funded in equal shares by the Federal Institute for Geosciences and Natural Resources (BGR) and IFREMER, whereas the KM14 expedition was funded by the BGR. The research leading to these results has received funding from the European Union Seventh Framework Programme (FP7/2007-2013) under the MIDAS project, grant agreement n° 603418.

Appendix A. Supplementary material

Supplementary information associated with this article can be found in the online version at doi:xxxxx.

References

Appeltans, W., Ahyong, S.T., Anderson, G., Angel, M.V., Artois, T., Bailly, N., Bamber, R., Barber, A., Bartsch, I., Berta, A., Błażewicz-Paszkowycz, M., et al., 2012. The magnitude of global marine species diversity. Current Biology 22(23), 2189–2202.

Baird, H.P., Miller, K.J., & Stark, J.S. 2011. Evidence of hidden biodiversity, ongoing speciation and diverse patterns of genetic structure in giant Antarctic amphipods. Molecular Ecology 20(16), 3439–3454. http://doi.org/10.1111/j.1365-294X.2011.05173.x.

Birstein, J.A., 1963. Deep-sea isopod crustaceans of the northwestern Pacific Ocean. Institute of Oceanology of the USSR, Akademii Nauk, Moscow, (in Russian with English summary).

Błażewicz-Paszkowycz, M., Jennings, R.M., Jeskulke, K., Brix, S., 2014. Discovery of swimming males of Paratanaoidea (Tanaidacea). Polish Polar Research 35(2), 415–453.

Bouckaert, R., Heled, J., Kühnert, D., Vaughan, T., Wu, C.-H., Xie, D., et al., 2014. BEAST 2: A Software Platform for Bayesian Evolutionary Analysis. PLoS Computational Biology 10(4), e1003537.

Brandt, A., Brix, S., Brökeland, W., Choudhury, M., Kaiser, S., Malyutina, M., 2007. Deep-sea isopod biodiversity, distribution and endemism in the Atlantic sector of the Southern Ocean – results from the ANDEEP I - III expeditions. Deep -Sea Research II 54, 1760–1775.

Brandt, A., Elsner, N., Brenke, N. Golovan, O., Malyutina, M.V., Riehl, T., Schwabe, E., Würzberg, L., 2013. Epifauna of the Sea of Japan collected via a new epibenthic sledge equipped with camera and environmental sensor systems. Deep -Sea Research II 86, 43–55.

Brandt, A., Brix, S., Held, C., Kihara, T.C., 2014. Molecular differentiation in sympatry despite morphological stasis: deep-sea *Atlantoserolis* Wägele, 1994 and *Glabroserolis* Menzies, 1962 from the south-west Atlantic (Crustacea: Isopoda: Serolidae). Zoological Journal of the Linnean Society 172(2), 318–359.

Brandt, A., Devey, C.W., Arndt, H., Riehl, T., this issue. Introduction to the bathymetry of the Vema-Fracture Zone and Puerto Rico TRench and Abyssal AtlaNtic BiodiverSITy Study (TRANSIT). Deep Sea Research Part II, this issue.

Brenke, N., 2005. An epibenthic sledge for operations on marine soft bottom and bedrock. Marine Technology Society Journal 39(2), 10–21.

Brix, S., Svavarsson, J., 2010. Distribution and diversity of desmosomatid and nannoniscid isopods (Crustacea) on the Greenland–Iceland–Faeroe Ridge. Polar Biology 33(4), 515–530.

Brix, S., Riehl, T., Leese, F., 2011. First genetic data for species of the genus *Haploniscus* Richardson, 1908 (Isopoda: Asellota: Haploniscidae) from neighbouring deep-sea basins in the South Atlantic. Zootaxa 2838, 79–84.

Brix, S., Leese, F., Riehl, T., Kihara, T.C., 2015. A new genus and new species of Desmosomatidae Sars, 1897 (Isopoda) from the eastern South Atlantic abyss described by means of integrative taxonomy. Marine Biodiversity 45(1), 7–61.

Brix, S., Bober, S., Tschesche, C., Kihara, T.C., Driskell, A., Jennings, R.M., this issue. Molecular species delimitation and its implications for species descriptions using desmosomatid and nannoniscid isopods from the VEMA fracture zone as example taxa, Deep Sea Research Part II, this issue.

Carstens, B.C., Pelletier, T.A., Reid, N.M., Satler, J.D., 2013. How to fail at species delimitation. Molecular Ecology 22(17), 4369–4383.

Dayrat, B., 2005. Towards integrative taxonomy. Biological Journal of the Linnean Society 85(3), 407–415.

De Queiroz, K., 2007. Species Concepts and Species Delimitation. Systematic Biology 56(6), 879–886.

Devey, C.W. (ed), 2015. RV SONNE Fahrtbericht / Cruise Report SO237 Vema-TRANSIT. Geomar Report 23, 130.

Drummond, A.J., Ho, S., Phillips, M.J., Rambaut, A., 2006. Relaxed Phylogenetics and Dating with Confidence. PLoS Biology 4(5), p.e88.

Etter, R.J., Rex, M.A., Chase, M.R., Quattro, J.M. 2005. Population differentiation decreases with depth in deep-sea bivalves. Evolution 59(7), 1479–1491.

Fujisawa, T., Barraclough, T.G., 2013. Delimiting Species Using Single-Locus Data and the Generalized Mixed Yule Coalescent Approach: A Revised Method and Evaluation on Simulated Data Sets. Systematic Biology 62(5), 707–724.

Gage, J.D., Tyler, P.A., 1992. Deep-sea biology: a natural history of organisms at the deep-sea floor. Cambridge University Press, Cambridge

George, R.Y., 2001. Desmosomatidae and Nannoniscidae (Crustacea, Isopoda, Asellota) from bathyal and abyssal depths off North Carolina and their evolution. Journal of Natural History 35(12), 1831–1859.

Guggolz ,T., Lins, L., Meißner, K., Brandt, A., this issue. Biodiversity and distribution of polychaetes (Annelida) in the Vema Fracture Zone. Deep Sea Research Part II, this issue.

Havermans, C., Sonet, G., d'Acoz, C.D.U., Nagy, Z.T., Martin, P., Brix, S., Riehl, T., Agrawal, S., Held, C., 2013. Genetic and morphological divergences in the cosmopolitan deep-sea amphipod *Eurythenes gryllus* reveal a diverse abyss and a bipolar species. PLoS One 8(9), p.e74218.

Hessler, R.R., 1970. The Desmosomatidae (Isopoda, Asellota) of the Gay Head-Bermuda transect. Bulletin of the Scripps Institution of Oceanography 15, 1–185.

Janssen, A., Kaiser, S., Meißner, K., Brenke, N., Menot, L., Arbizu, P.M., 2015. A reverse taxonomic approach to assess macrofaunal distribution patterns in abyssal Pacific polymetallic nodule fields. PloS one 10(2), p.e0117790.

Jennings, R.M., Etter, R.J., Ficarra, L., 2013. Population differentiation and species formation in the deep sea: the potential role of environmental gradients and depth. PLoS One. http://doi.org/10.1371/journal.pone.0077594.

Johnson, S.B., Young, C.R., Jones, W.J., Warén, A., Vrijenhoek, R.C., 2006. Migration, isolation, and speciation of hydrothermal vent limpets (Gastropoda; Lepetodrilidae) across the Blanco Transform Fault. The Biological Bulletin 210(2), 140–157. http://doi.org/10.2307/4134603.

Jones, G.R., 2014. STACEY: Species delimitation and phylogeny estimation under the multispecies coalescent. bioRxiv, 1–7.

Kaiser, S., 2014. New species of *Hebefustis* Siebenaller & Hessler 1977 (Isopoda, Asellota, Nannoniscidae) from the Clarion Clipperton Fracture Zone (equatorial NE Pacific). Zootaxa 3784(2), 101–119.

Kaiser, S., 2015. A new species of *Regabellator* Siebenaller & Hessler, 1981 (Isopoda, Asellota, Nannoniscidae) from the Amundsen Sea shelf (Southern Ocean). Crustaceana 88(4), 405–421.

Kaiser, S., Barnes, D.K.A., Sands, C.J., Brandt, A., 2009. Biodiversity of an unknown Antarctic Sea: assessing isopod richness and abundance in the first benthic survey of the Amundsen continental shelf. Marine Biodiversity 39(1), 27–43.

Kaiser, S., Brenke, N., 2016. Epibenthic sledges, in: Clark, M.R., M. Consalvey, A.A. Rowden (Eds.), Biological Sampling in the Deep Sea, Wiley-Blackwell, pp. 184–206.

Katoh, K., Standley, D.M., 2013. MAFFT Multiple Sequence Alignment Software Version 7: Improvements in Performance and Usability. Molecular Biology and Evolution 30(4), 772–780.

Kihara, T.C., Rocha, C.E.F., 2009. Técnicas para Estudo Taxonômico de Copépodes Harpacticóides da Meiofauna Marinha. Asterisco, São Paulo 96.

Larkin, M.A., Blackshields, G., Brown, N.P., Chenna, R., McGettigan, P.A., McWilliam, H., et al., 2007. Clustal W and Clustal X version 2.0. Bioinformatics 23(21), 2947–2948.

Lim, G.S., Balke, M., Meier, R., 2012. Determining species boundaries in a world full of rarity: singletons, species delimitation methods. Systematic Biology 61(1), 165–169.

Lins, L.S., Ho, S.Y., Wilson, G.D.F., Lo, N., 2012. Evidence for Permo-Triassic colonization of the deep sea by isopods. Biology Letters, p.rsbl20120774.

Lohse, K., 2009. Can mtDNA barcodes be used to delimit species? A response to Pons et al. (2006). Systematic Biology 58(4), 439–442.

McClain, C.R., Rex, M.A., Etter, R.J., 2009. Deep-sea macroecology, in: Witman, J.D., Roy, K. (Eds.), Marine macroecology, Chicago, IL, University of Chicago Press, pp. 65–100.

Merrin, K., 2014. Janiroidea Sars, 1897. in: Boyko, C.B., Bruce, N.L., Merrin, K.L., Ota, Y., Poore, G.C.B., Taiti, S., Schotte, M., Wilson, G.D.F. (Eds.) (2008 onwards). World Marine, Freshwater and Terrestrial Isopod Crustaceans database. http://www.marinespecies.org/aphia.php?p=taxdetails&id=155716 (accessed 21.07.2016)

Michels, J., Büntzow, M., 2010. Assessment of Congo red as a fluorescence marker for the exoskeleton of small crustaceans and the cuticle of polychaetes. Journal of Microscopy 238, 95–101.

Mora, C., Tittensor, D.P., Adl, S., Simpson, A.G., Worm, B., 2011. How many species are there on Earth and in the ocean? PLoS Biology 9(8), p.e1001127.

Passamonti, M., Ghiselli, F., 2009. Doubly uniparental inheritance: two mitochondrial genomes, one precious model for organelle DNA inheritance and evolution. DNA and Cell Biology 28(2), 79–89.

Pons, J., Barraclough, T., Gomez-Zurita, J., Cardoso, A., Duran, D., Hazell, S., et al., 2006. Sequence-Based Species Delimitation for the DNA Taxonomy of Undescribed Insects. Systematic Biology 55(4), 595–609.

Puillandre, N., Lambert, A., Brouillet, S., Achaz, G., 2012. ABGD, Automatic Barcode Gap Discovery for primary species delimitation. Molecular Ecology 21(8), 1864–1877.

QGIS Development Team, 2015. QGIS Geographic Information System. Open Source Geospatial Foundation Project. Available at: http://qgis.osgeo.org.

Rambaut, A., Suchard, M.A., Xie, D., Drummond, A.J., 2014. Tracer v1. 6.

Rannala B., Yang Z. (2013) Improved reversible jump algorithms for Bayesian species delimitation. Genetics 194, 245–253.

Raupach, M.J., Held, C., Wägele, J.-W., 2004. Multiple colonization of the deep sea by the Asellota (Crustacea: Peracarida: Isopoda). Deep-Sea Research Part II 51, 1787–1795.

Raupach, M.J., Malyutina, M., Brandt, A., Wägele, J.W., 2007. Molecular data reveal a highly diverse species flock within the munnopsoid deep-sea isopod *Betamorpha fusiformis* (Barnard, 1920)

(Crustacea: Isopoda: Asellota) in the Southern Ocean. Deep Sea Research Part II 54(16), 1820–1830.

Riehl, T., Brandt, A., 2010. Descriptions of two new species in the genus *Macrostylis* Sars, 1864 (Isopoda, Asellota, Macrostylidae) from the Weddell Sea (Southern Ocean), with a synonymisation of the genus *Desmostylis* Brandt, 1992 with *Macrostylis*. Zookeys 57, 9–49.

Riehl, T., Kaiser, S., 2012. Conquered from the deep sea? A new deep-sea isopod species from the Antarctic shelf shows pattern of recent colonization. PLoS ONE 7(11), p.e49354.

Riehl, T., Wilson, G.D.F., Hessler, R.R., 2012. New Macrostylidae Hansen, 1916 (Crustacea: Isopoda) from the Gay Head-Bermuda transect with special consideration of sexual dimorphism. Zootaxa 3277, 1–26.

Riehl, T., Brenke, N., Brix, S., Driskell, A., Kaiser, S., Brandt, A., 2014a. Field and Laboratory Methods for DNA Studies on Deep-sea Isopod Crustaceans. Polish Polar Research 35(2), 203–224.

Riehl, T., Wilson, G.D.F., Malyutina, M.V., 2014b. Urstylidae–a new family of abyssal isopods (Crustacea: Asellota) and its phylogenetic implications. Zoological Journal of the Linnean Society 170(2), 245–296.

Riehl, T., Lins, L., Brandt, A., this issue. The effects of depth, distance, and the Mid-Atlantic Ridge on genetic differentiation of abyssal and hadal isopods (Macrostylidae). Deep Sea Research Part II, this issue.

Schotte, M., Kensley, B.F., Shilling, S., 2009. World list of Marine, Freshwater and Terrestrial Crustacea Isopoda. National Museum of Natural History Smithsonian Institution: Washington D.C., USA. World Wide Web electronic publication. Available online at http://www.nmnh.si.edu/iz/isopod/. Accessed July 2016.

Schüller, M., 2011. Evidence for a role of bathymetry and emergence in speciation in the genus *Glycera* (Glyceridae, Polychaeta) from the deep Eastern Weddell Sea. Polar Biology 34(4), 549–564.

Talavera, G., Castresana, J., 2007. Improvement of phylogenies after removing divergent and ambiguously aligned blocks from protein sequence alignments. Systematic biology 56(4), 564–577.

Tyler, P.A., Baker, M., Ramirez-Llodra, E., 2016. Deep-Sea Benthic Habitats, in: Clark, M.R., M. Consalvey, A.A. Rowden (Eds.), Biological Sampling in the Deep Sea, Wiley-Blackwell, pp. 1–15.

Wägele, J.W., 1989. Evolution und phylogenetisches System der Isopoda. Zoologica 140, 262 pp.

Wilson, G.D., 1998. Historical influences on deep-sea isopod diversity in the Atlantic Ocean. Deep Sea Research Part II 45(1), 279–301.

Wilson, G.D.F., 1999. Some of the deep-sea fauna is ancient. Crustaceana 72(8), 1019–1030.

Wilson, G.D.F., 2008. A review of taxonomic concepts in the Nannoniscidae (Isopoda, Asellota), with a key to the genera and a description of *Nannoniscus oblongus* Sars. Zootaxa 1680, 1–24.

Wolff, T., 1962. The systematics and biology of bathyal and abyssal Isopoda Asellota. Danish Science Press, 7–320.

Yang, Z., Rannala, B., 2010. Bayesian species delimitation using multilocus sequence data. Proceedings of the National Academy of Sciences 107(20), 9264–9269.

Zhang, J., Kapli, P., Pavlidis, P., Stamatakis, A., 2013. A general species delimitation method with applications to phylogenetic placements. Bioinformatics 29(22), 2869–2876.

Figure captions

Fig. 1 Global distribution of *Ketosoma* and *Thaumastosoma* species; 1) *Ketosoma distinctum* (Birstein, 1963) *comb. nov.;* 2, 3) *Thaumastosoma platycarpus* Hessler, 1970, *Thaumastosoma tenue* Hessler, 1970; 4) *Thaumastosoma* cf. *platycarpus* (IDesm010_ICE- IDesm046_ICE); 5-7) *Ketosoma ruehlemanni* sp. nov., *Ketosoma* sp. 1 (NB12_Iso740_9); *Ketosoma* sp. 2 (KM14_Iso259_1); 8) *Ketosoma jebamoni* (George, 2001) comb. nov.; 9) *Ketosoma hessleri* sp. nov.; 10) *Ketosoma vemae*

sp. nov; 11, 12) *Thaumastosoma diva* sp. nov.; *Ketosoma werneri* sp. nov. The sampling location for *K. distictum* has been inferred from the expedition route reported by Birstein (1963), but does not reflect the precise station. Dashed line indicates the equator.

Fig. 2 Multilocus Bayesian tree and species delimitation results. Phylogenetic scale denotes evolutionary distance among taxa based on all three markers. Numbers above branches indicate Bayesian posterior probabilities. Colored boxes indicate species delimitations from four "discovery" methods, and numbers below branches denote "validation" BPP posterior probabilities that the two directly descendant branches denote separate species, assuming the Bayesian tree topology as fixed.

Fig. 3 *Thaumastosoma platycarpus* Hessler, 1970, confocal laser scanning microscopy images; paratype, female (Australian Museum, P.59254); a, habitus, dorsal view; b, habitus, lateral view; c, habitus, ventral view; d, pereonite 7 and Plt, ventral view. Scale bars: a–c = 400 μm, d = 200 μm.

Fig. 4 *Thaumastosoma platycarpus* Hessler, 1970, confocal laser scanning microscopy images, paratype, male (Australian Museum, P.59254); a, habitus, dorsal view; b, habitus, lateral view; c, habitus, ventral view; d, pereonite 7 and Plt, ventral view. Scale bars: a–c = 400 μm, d = 200 μm.

Fig. 5 *Thaumastosoma tenue* Hessler, 1970; a–c, holotype female (USNM 125113), d–f, paratype female (Australian Museum, P.59256); a, habitus, dorsal view; b, cephalothorax, lateral view; c, habitus, lateral view; d, e, lMd, detail: molar process, incisor process and lacinia mobilis; f, Mx2. Scale bars: a, c = 1 mm, d–f = 100 μm.

Fig. 6 *Thaumastosoma tenue* Hessler, 1970, confocal laser scanning microscopy images; paratype, female (Australian Museum, P.59256); a, habitus, dorsal view; b, habitus, lateral view; c, pereonite 7 and Plt, ventral view. Scale bars: a–b = 400 μm, c = 200 μm.

Fig. 7 *Thaumastosoma diva* sp. nov.; a–e, holotype, female (ZMH K 46132); a, habitus, dorsal view; b, A1 and A2, drawn *in situ*; c, PI, drawn *in situ*; d, Mx2; e, Plp 1. Scale bars: a = 200 μm, b–e = 100 μm.

Fig. 8 *Thaumastosoma diva* sp. nov., confocal laser scanning microscopy images; holotype, male (ZMH K 46132); a, habitus, dorsal view; b, habitus, lateral view; c, habitus, ventral view; d, A1, dorsal view; e, mouthparts, ventral view. Scale bars: a–c = 200 μm, d = 50 μm, e = 100 μm.

Fig. 9 *Ketosoma ruehlemanni* sp. nov.; a, c, holotype, female (ZMH K 46133), b, d–h, paratype female (ZMH K 46135); a, habitus, dorsal view; b, A1; c, habitus, lateral view; d, Mx1; e, Mx2; f, rMd, detail: incisor process and mandible palpus; g, lMd; h, Mxp. Scale bars: a, c = 1 mm, b, d–h = 100 μm.

Fig. 10 *Ketosoma ruehlemanni* sp. nov.; a, b, holotype, female (ZMH K 46133), c–h, l–m, paratype, female (ZMH K 46135), i–k paratype, female (ZMH K 46136); a, habitus, lateral view; b, habitus, ventral view; c, Op; d, Plp 3; e, Plp 4; f, Plp 5; g, Urp; h–k, P 1–4; l–m, P 6–7. Scale bars: a, b = 1 mm, c = 200 μm , d–m = 100 μm.

Fig. 11 *Ketosoma ruehlemanni* sp. nov.; a, d–e, paratype, male (ZMH K 46139), b–c, paratype, male (ZMH K 46138). a, habitus, lateral view; b, Plp 2; c, Plp 1; d, Plt, ventral view; e, habitus, dorsal view. Scale bars: a, e = 200 μm, b, d–h = 100 μm.

Fig. 12 *Ketosoma ruehlemanni* sp. nov., confocal laser scanning microscopy images, paratype, male (ZMH K 46139); a, habitus, dorsal view; b, habitus, lateral view; c, habitus, ventral view; d,

mouthparts, ventral view; e, Plt, ventral view; f, cephalothorax, lateral view. Scale bars: a–b = 400 μm, c = 800 μm, d–f = 200 μm.

Fig. 13 *Ketosoma hessleri* sp. nov.; a–e, holotype, female (ZMH K 46141); a, habitus, dorsal view; b, cephalothorax, A1 and A2; c, habitus, lateral view; d, cephalothorax, lateral view; e, PI. Scale bars: a–d = 1 mm, e = 100 μm.

Fig. 14 *Ketosoma hessleri* sp. nov.; a–f, holotype, female (ZMH K 46141); a, lMd; b, Mx2; c, Mxp endite; d, Mxp palpus; e, PVI; detail: propodus, dactylus and ungius; f, habitus, lateral view. Scale bars: a–e = 100 μm, f = 1 mm.

Fig. 15 *Ketosoma vemae* sp. nov.; a–d, holotype, male (ZMH K 46140); a, habitus, dorsal view; b, cephalothorax, lateral view; c, cephalothorax, frontal view; d, habitus, lateral view. Scale bars: a = 400 μm, d = 200 μm.

Fig. 16 *Ketosoma vemae* sp. nov.; a–g, holotype, male (ZMH K 46140); a, A1; b, Md palpus; c, Mxp palpus; d, PIII; e, PIV; f, PV; g, right PI; h, left PI. Scale bars: a–h = 100 μm.

Fig. 17 *Ketosoma hessleri* sp. nov., confocal laser scanning microscopy images; holotype, female (ZMH K 46141); a, habitus, dorsal view; b, habitus, lateral view; c, Plt, ventral view; *Ketosoma vemae* sp. nov., holotype, male (ZMH K 46140); d, habitus, dorsal view; e, habitus, lateral view; f, cephalothorax, lateral view. Scale bars: a–b, d = 400 μm; c, e–f = 200 μm.

Fig. 18 *Ketosoma werneri* sp. nov.; a–h, holotype, female (ZMH K 46142); a, habitus, dorsal view; b, A1 and A2; c, habitus, posterior pereonites, lateral view; d, habitus, dorsal view; e, Op; f, PI; g, PIV; h, PVI. Scale bars: a–h = 100 μm.

Fig. 19 *Ketosoma werneri* sp. nov., confocal laser scanning microscopy images; holotype, female (ZMH K 46142); a, habitus, dorsal view; b, habitus, lateral view; c, mouthparts, ventral view; d, pereonite 7 and Plt, ventral view. Scale bars: a–d = 200 μm.

Table 1 Station list of sampling campaigns, where examined specimens were collected (including gear type, date, position (decimal degrees) and depth [m]); ARG: Argentine Basin; CCZ: Clarion Clipperton Fracture Zone; IB: Iceland Basin; NEA: North-East Atlantic.

Expedition	Area	Gear	Station	Date	Start lat	Start long	End lat	End long	Depth [m]
BIONOD	CCZ	EBS	#06	02/04.2012	11.770346'N	116.68556'W	11.770360'N	116.68551'W	4259
BIONOD	CCZ	EBS	#33	07/04/2012	11.862434'N	117.052893'W	11.8651339'N	117.052225'W	4133
BIONOD	CCZ	EBS	#43	09/04/2012	11.803588'N	117.53435'W	11.8056938'N	117.532522'W	4358
KM14	CCZ	EBS	#20	10/05/2014	11.864722'N	117.020556'W	11.869722'N	117.008611'W	4127-4124
DIVA 3	ARG	EBS	#534	16/07/2009	36.01016'S	49.02566'W	36.0115'S	49.029'W	4608
VEMA	NEA	C-EBS	#2-6	20/12/2014	10.709167'N	25.0994'W	10.7266667`N	25.0866667'W	5520
VEMA	NEA	C-EBS	#6-7	02/01/2015	10.351389'N	36.9502778'W	10.3652778'N	36.9327778'W	5085–5079
IceAge	IB	EBS	963	28/08/2011	60.0455'N	21.46766`W	60.0455'N	21.498'W	2749.4
IceAge	IB	RP Sled	967	29/08/2011	60.04616'N	21.47566'W	60.04633'N	21.50116'W	2750.4

Table 2 List of voucher specimens used for molecular-genetic analyses. All voucher specimens are located at the CeNak Hamburg (ZMH catalogue). ARG: Argentine Basin; CB: Cape Basin; GB: Guinea Basin; IB: Iceland Basin; NEA: North-East Atlantic; CCZ: Clarion Clipperton Fracture Zone.

Voucher identification #	Expedition	Area	Station	Taxon (type status)	Marker	GenBank accession #	ZMH catalogue #	Sex
D2D003	DIVA2	CB	40/1	*Chelator rugosus* (paratype)	COI, 16S, 18S	KJ578686 KJ578667 KJ578678	K 43229	M
D2D051	DIVA2	GB	90/7	*Chelator aequabilis* (paratype)	COI, 16S, 18S	KJ578690 KJ578663 KJ578675	K 43205	j.
IDesm014	IceAge	IB	967	*Chelator vulgaris*	COI, 16S, 18S	KJ710289 KJ630813 KJ630816	K 19860	n.a.
IDesm010_ICE	IceAge	IB	967	*Thaumastosoma* cf. *platycarpus*	COI, 16S, 18S	MF040897 KY951735 KY951740	K 46143	F
IDesm012_ICE	IceAge	IB	967	*Thaumastosoma* cf. *platycarpus*	COI, 16S	MF040896 KY951734	K 46144	F
IDesm041_ICE	IceAge	IB	963	*Thaumastosoma* cf. *platycarpus*	COI, 16S	MF040895 KY951733	K 46145	F
IDesm045_ICE	IceAge	IB	963	*Thaumastosoma* cf. *platycarpus*	COI, 16S	MF040894 KY951732	K 46146	M
IDesm046_ICE	IceAge	IB	963	*Thaumastosoma* cf. *platycarpus*	COI, 16S	MF040898 KY951736	K 46147	F
D3D060	DIVA 3	ARG	534	*Ketosoma werneri* sp. nov. (holotype)	COI, 18S	MF040893 KY951738	K 46142	F
D3D064	DIVA 3	ARG	534	*Thaumastosoma diva* sp. nov. (holotype)	16S, 18S	KY951731 KY951739	K 46132	M
VTDesm013	Vema	NEA	2-6	*Ketosoma vemae* sp. nov. (holotype)	COI, 16S, 18S	MF040892 KY951730 KY951737	K 46140	M
VTDesm569	Vema	NEA	6-7	*Ketosoma hessleri* sp. nov. (holotype)	16S	KY951729	K 46141	F
NBIso337	BIONOD	CCZ	43	*Ketosoma ruehlemanni* sp. nov. (paratype)	COI	KJ736158	K 46139	M
NB12_Iso740_9	BIONOD	CCZ	06	*Ketosoma* sp. nov. 1	18S	KY693696	K 46148	M
KM14_Iso259_1	KM14	CCZ	20	*Ketosoma* sp. nov. 2	COI, 16S, 18S	KY693699 KY693698 KY693694	K 46149	F
KM14_Iso261_2	KM14	CCZ	20	*Ketosoma* sp. nov. 2	16S, 18S	KY693697 KY693695	K 46150	F

Table 3 Confocal laser scanning microscopy (CLSM) settings. Ch1 and Ch2 = detection channels 1 and 2.

Numerical aperture	0.4
Excitation beam splitter	DD 488/561
Detected emission wavelength (nm)	Ch1: 570 - 629
	Ch2: 629 - 717
Detector gain	544 and 509 V
Amplitude offset	-1.7 and -0.8 %
Pinhole aperture (µm)	53.0

Table 4 ABGD 16S pairwise uncorrected p-distances between specimens investigated. For 16S ABGD analysis detected a barcode gap between 1% and 4% pairwise difference, noteworthy values are shown in bold.

		1	2	3	4	5	6	7	8	9	10	11	12	13
1	D2D003_ *Chelator rugosus*													
2	D2D051_*Chelator aequabilis*	0.16 16												
3	D3D064_*Thaumastosoma diva* sp. nov.	0.33 5	0.34 53											
4	IDesm010_ICE_*Thaumastosoma* cf. *platycarpus*	0.29 38	0.29 79	0.20 05										

5	IDesm012_ICE_ *Thaumastosoma* cf. *platycarpus*	0.2964	0.3005	0.2024	**0.0047**								
6	IDesm014_ICE_*Chelator insignis*	0.1797	0.1823	0.3138	0.2912	0.2912							
7	IDesm041_ICE_ *Thaumastosoma* cf. *platycarpus*	0.2964	0.3005	0.2005	**0.0047**	**0**	0.2912						
8	IDesm045_ICE_ *Thaumastosoma* cf. *platycarpus*	0.2964	0.3005	0.2024	**0.0047**	**0**	0.2912	**0**					
9	IDesm046_ICE_ *Thaumastosoma* cf. *platycarpus*	0.2946	0.3013	0.198	**0.0073**	**0.0048**	0.2894	**0.0024**	**0.0048**				
10	KM14_Iso259_1 *Ketosoma* sp. 2	0.2872	0.2962	0.2453	0.2033	0.2028	0.2814	0.2033	0.2028	0.2112			
11	KM14_Iso261_2 *Ketosoma* sp. 2	0.2872	0.2962	0.2441	0.2033	0.2028	0.2814	0.2033	0.2028	0.2112	**0**		
12	VT569_*Ketosoma hessleri* sp. nov.	0.273	0.2769	0.2423	0.2251	0.227	0.2769	0.2251	0.227	0.2315	0.1248	0.1216	
13	VTDes013_ *Ketosoma vemae* sp. nov.	0.2806	0.2821	0.2463	0.2251	0.2246	0.2769	0.2251	0.2246	0.234	0.1187	0.1187	**0.0541**

Table 5 ABGD COI pairwise uncorrected p-distances between specimens investigated

		1	2	3	4	5	6	7
1	D2D003 *Chelator rugosus*							
2	D2D051 *Chelator aequabilis*	0.154						
3	D3D060 *Ketosoma werneri* sp. nov.	0.3533	0.3786					
4	IDesm014 *Chelator insignis*	0.246	0.244	0.3175				
5	KM14_Iso259_1 *Ketosoma* sp. 2	0.3601	0.3694	0.1847	0.3274			
6	VTDesm013 *Ketosoma vemae* sp. nov.	0.3551	0.3551	0.1656	0.3095	0.194		
7	NBIso337 *Ketosoma ruehlemanni* sp. nov.	0.3406	0.3279	0.1589	0.3095	0.1679	0.1689	

Table 6 Morphological comparison of species within *Thaumastosoma* and *Ketosoma* gen. nov.**;** characters were also examined from undescribed species included in the molecular-genetic analysis (voucher KM14Iso259_1, KM14Iso261_2, and NB12Iso740_9); an asterisk indicates synapomorphies shared between *Ketosoma* species.

Character	*T. platycarpus*	*T. tenue*	*T. diva sp. nov.*	*K. distinctum comb. nov.*	*K. ruehlemanni sp. nov.*	*K. vemae sp. nov.*	*K. hessleri sp. nov.*	*KM14 Iso259_1*	*KM14 Iso261_2*	*NB12 Iso740_9*	*K. werneri sp. nov.*	*K. jebamoni comb. nov.*
Gender	M/F	F	M	F	F	M	F	F	F	M	F	F
A1, number articles	6	6	6	6	13	11	13	13	damaged	11	6	11
mouth parts	produced forward, elongated	produced forward, elongated	produced forward, elongated	?	produced forward, elongated	produced forward, elongated	produced forward, elongated	produced forward, elongated	produced forward, elongated	produced forward, elongated	produced forward, elongated	n.a.
Mxp, coupling hooks	unusually long coupling hooks	unusually long coupling hooks	unusually long coupling hooks	unusually long coupling hooks	unusually long coupling hooks	unusually long coupling hooks	unusually long coupling hooks	n.a.	n.a.	n.a.	unusually long coupling hooks	n.a.
Mxp palpal article 3	medial setae arranged in an arc on the ventral surface	medial setae arranged in an arc on the ventral surface	medial setae arranged in an arc on	medial setae located in an arc on the ventral surface	medial setae inserting at the distal margin	medial setae arranged in an arc on the ventral surface	medial setae inserting at the distal margin	n.a.	n.a.	n.a.	medial setae inserting at the distal margin	n.a.

	of the segment	of the segment	the ventral surface of the segment	of the segment		of the segment						
Mx2*	mesial endite reduced	mesial endite reduced	mesial endite reduced	n.a.	not reduced	n.a.	n.a.	n.a.	n.a.	n.a.	n.a.	n.a.
First pereonite*	robust seta on coxa	robust seta on coxa	robust seta on coxa	seta on tergite	robust seta on tergite	robust seta on tergite	robust seta on tergite	robust seta on tergite	robust seta on tergite	robust seta on tergite	robust seta on tergite	no seta drawn
Ventral spine pereonite 7*	present	present	n.a.	n.a.	absent	absent	absent	absent	absent	absent	absent	n.a.
Plt	with pair of very poorly developed posterolateral angularities in female	with pair of very poorly developed posterolateral angularities in female	n.a.	with well developed posterolateral spines in female	with well developed posterolateral spines in female, similar to male	with well developed posterolateral spines in male	with well developed posterolateral spines in female	with well developed posterolateral spines in female	with well developed posterolateral spines in female	n.a.	with well developed posterolateral spines in female	with well developed posterolateral spines in female
Female operculum*	with ventral spine	with ventral spine	n.a.	without ventral spine	without ventral spine	n.a.	without ventral spine	without ventral spine	without ventral spine	n.a.	without ventral spine	without ventral spine

Table 7 Checklist of species within *Ketosoma* gen. nov. and *Thaumastosoma* Hessler, 1970 including information on their type locality

Species	Type locality	Lat/long (decimal degree)	Depth (m)
Ketosoma gen. nov.			
K. distinctum (Birstein, 1963) comb. nov.	NW Pacific	n.a.	5680–5690
K. jebamoni (George, 2001) comb. nov.	NW Atlantic	33.33333` - 33.333889'N, 71.516667` - 71.51722`W	5325
K. ruehlemanni gen. et sp. nov.	Equatorial NE Pacific	11.862434 - 11.803588'N, 117.05289 -117.53435'W	4133–4358
K. vemae gen. et sp. nov.	Equatorial NE Atlantic	10.709167' - 10.72667`N, 25.0994' - 25.086667'W	5520
*K. hessler*i gen. et sp. nov.	Equatorial NE Atlantic	10.351389' - 10.36528'N, 36.950278' - 36.932778'W	5085– 5079
K. werneri gen. et sp. nov.	SE Atlantic	36.01016'S, 49.02566'W	4608
Thaumastosoma Hessler, 1970			
T. diva sp. nov.	SW Atlantic	36.01016'S, 49.02566'W	4608
T. platycarpus Hessler, 1970	N Atlantic	38.7667'N, 70.1000`W	2886
T. tenue Hessler, 1970	N Atlantic	38.7667'N, 70.1000`W	2886

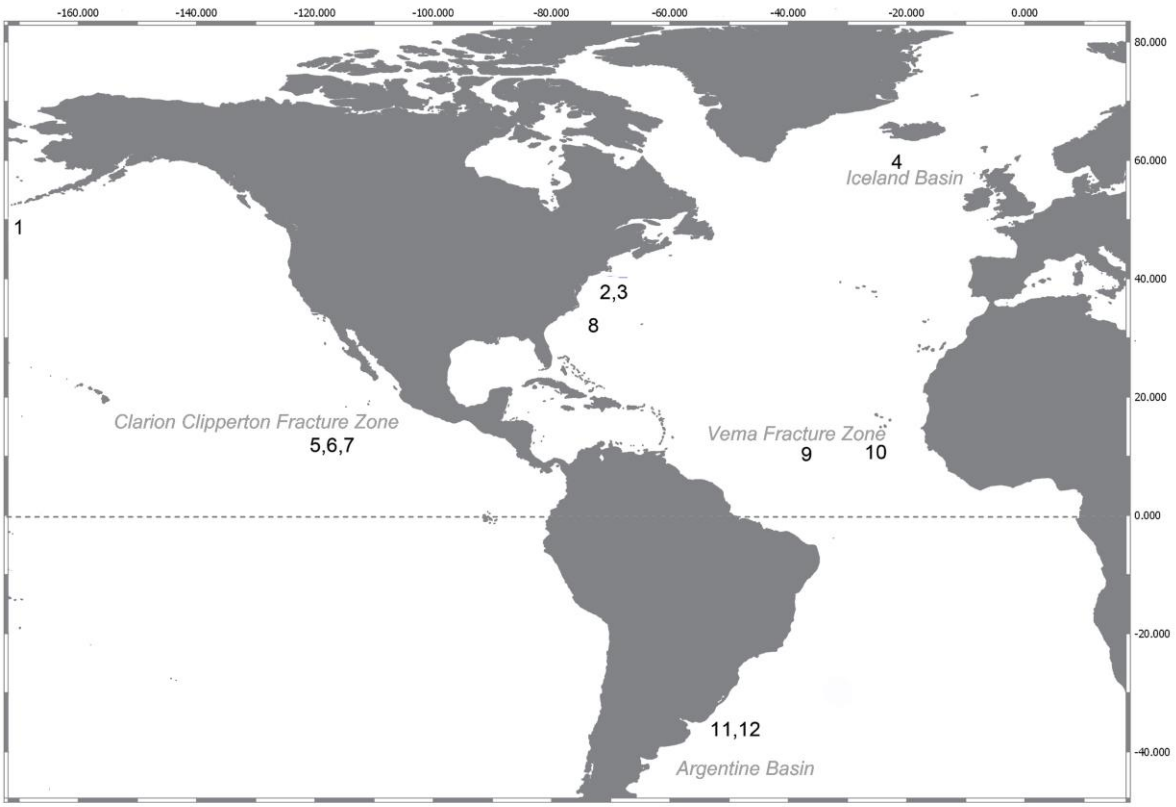
-160.000
-140.000
-120.000
-100.000
-80.000
-60.000
-40.000
-20.000
0.000
80.000
60.000
40.000
20.000
0.000
-20.000
-40.000
1
2,3
8
4
Iceland Basin
Clarion Clipperton Fracture Zone
5,6,7
Verna Fracture Zone
9
10
11,12
Argentine Basin

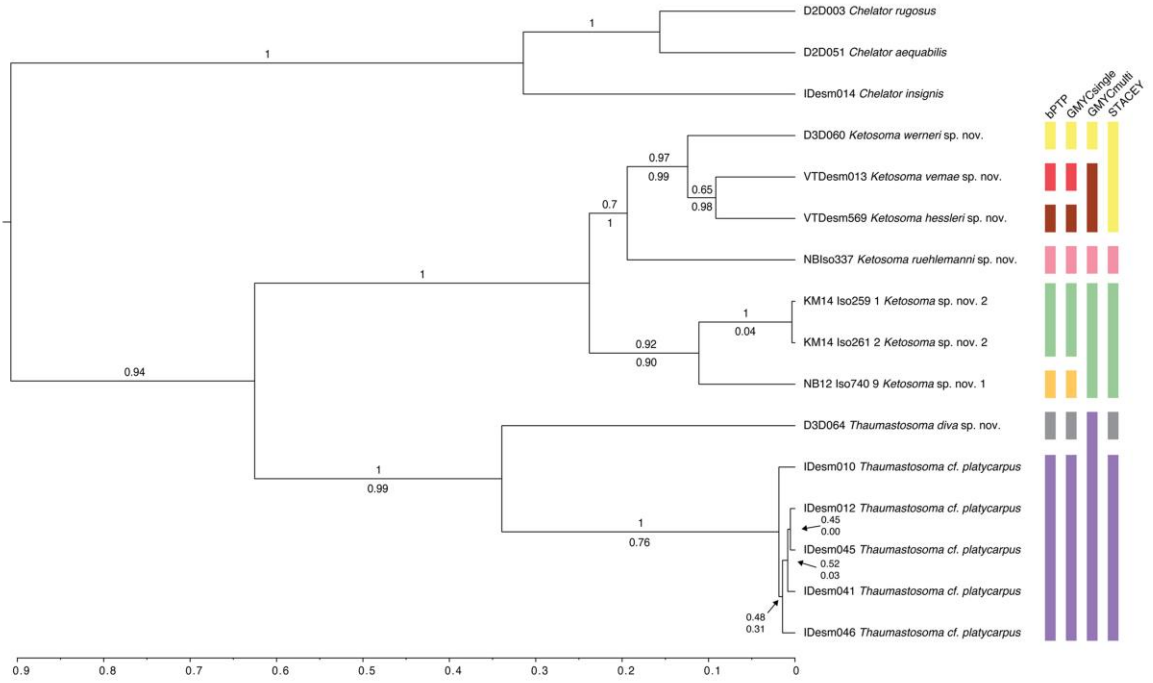
D2D003 Chelator rugosus
D2D051 Chelator aequabilis
IDesm014 Chelator insignis
D3D060 Ketosoma werneri sp. nov.
VTDesm013 Ketosoma vemae sp. nov.
VTDesm569 Ketosoma hessleri sp. nov.
NBIso337 Ketosoma ruehlemanni sp. nov.
KM14 Iso259 1 Ketosoma sp. nov. 2
KM14 Iso261 2 Ketosoma sp. nov. 2
NB12 Iso740 9 Ketosoma sp. nov. 1
D3D064 Thaumastosoma diva sp. nov.
IDesm010 Thaumastosoma cf. platycarpus
IDesm012 Thaumastosoma cf. platycarpus
IDesm045 Thaumastosoma cf. platycarpus
IDesm041 Thaumastosoma cf. platycarpus
IDesm046 Thaumastosoma cf. platycarpus
bPTP
GMYCsingle
GMYCmulti
STACEY
0.9
0.8
0.7
0.6
0.5
0.4
0.3
0.2
0.1
0

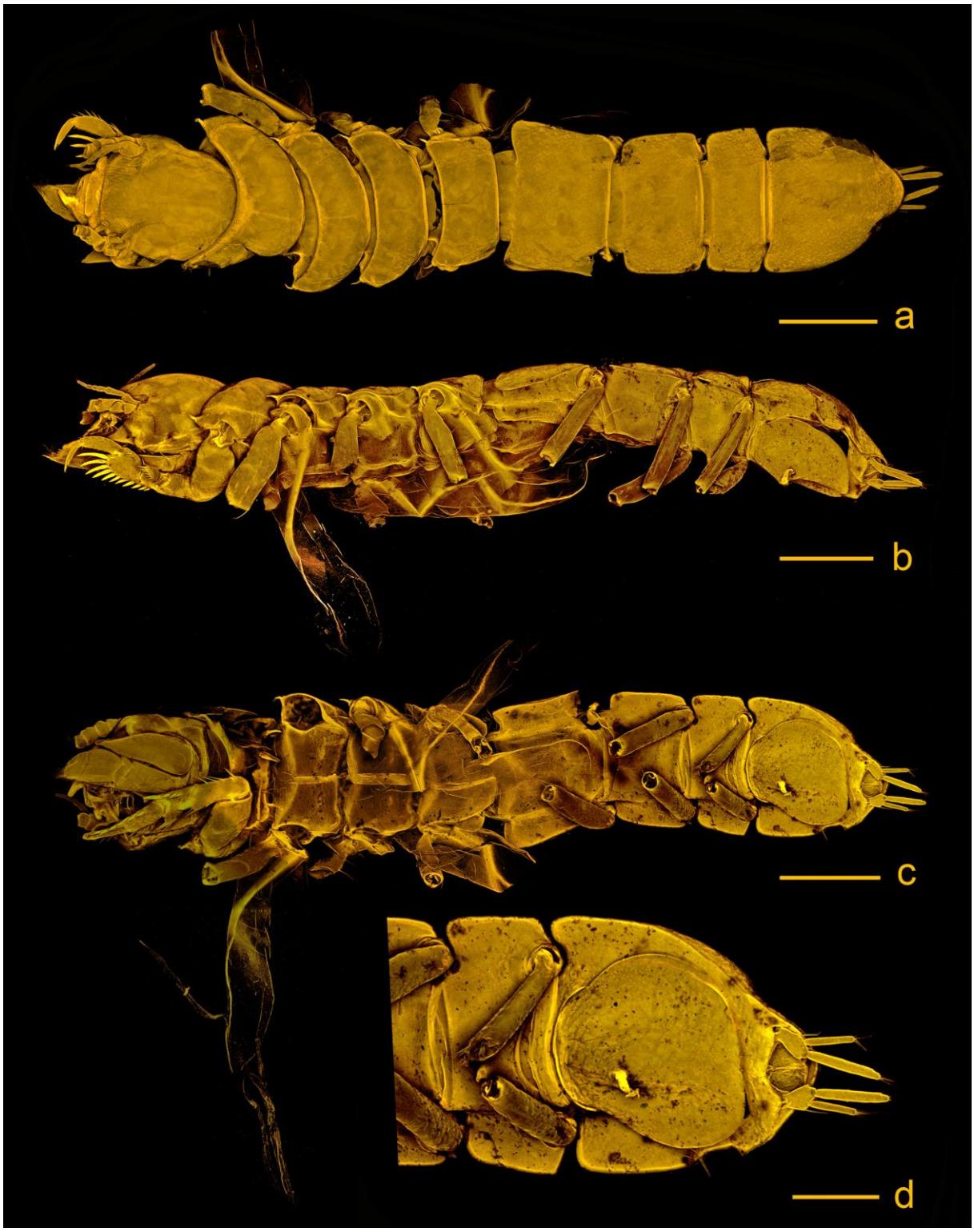
a
b
c
d


a
b
c
d

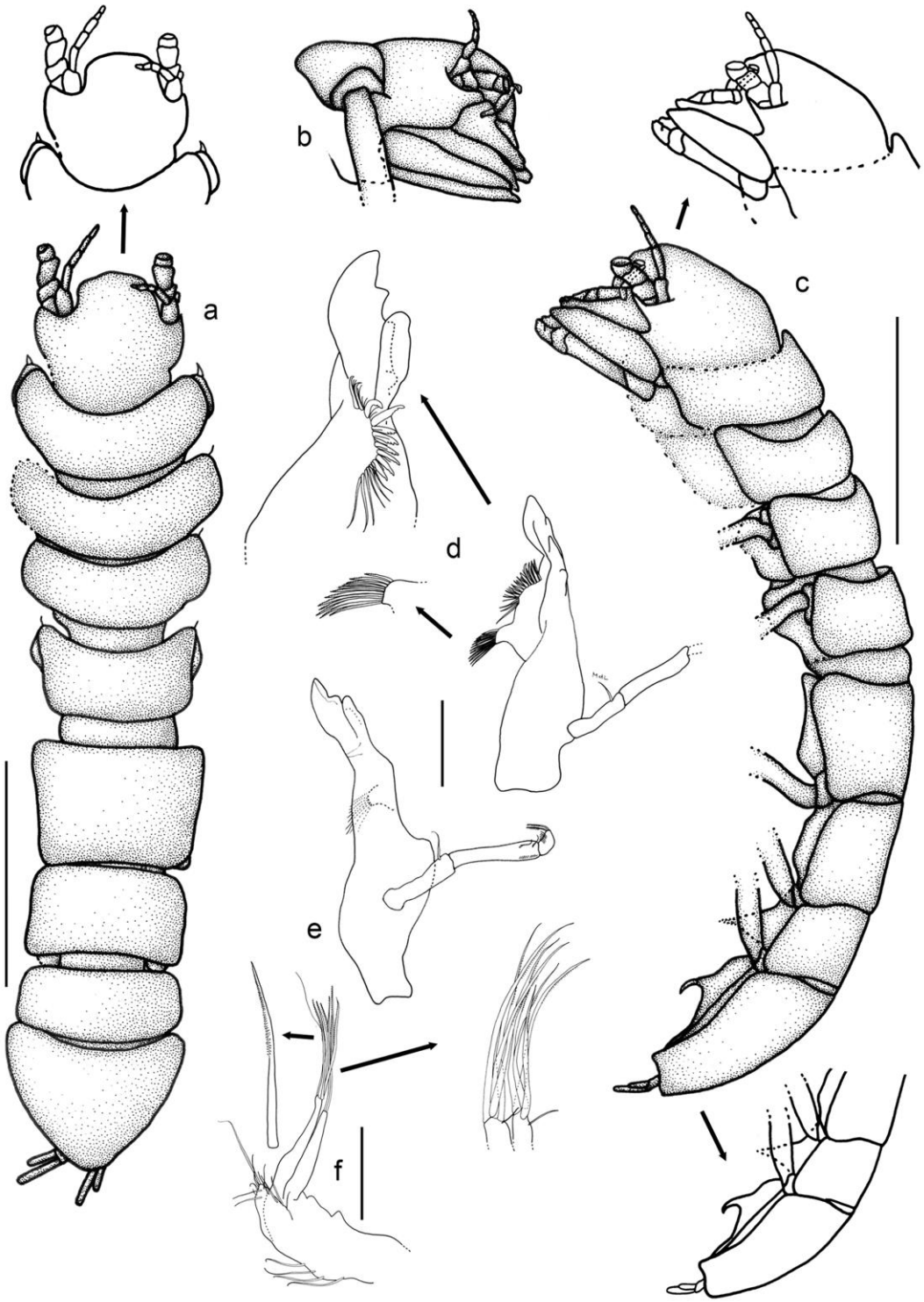
a
b
c
d
e
f


a
b
c

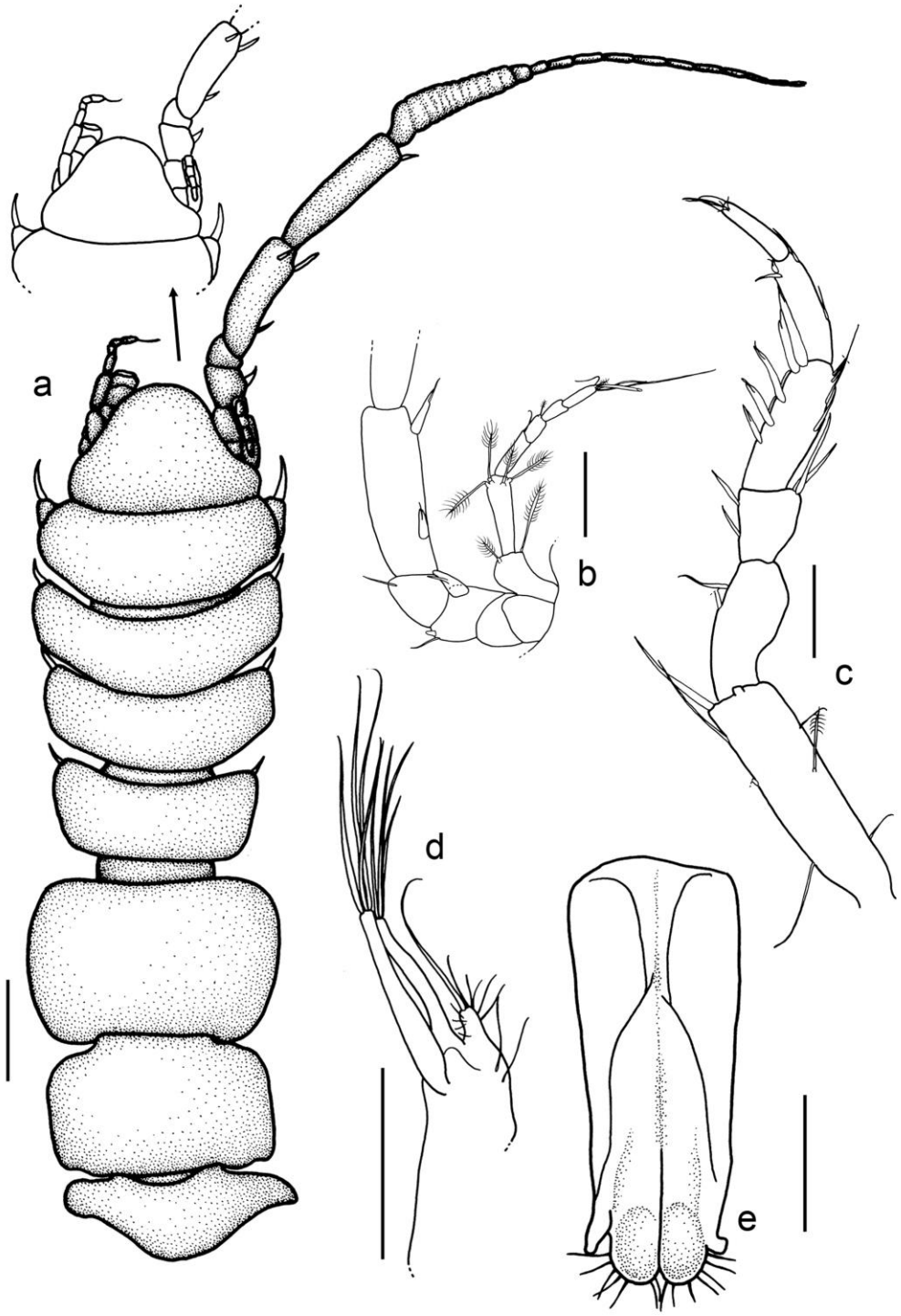
a
b
c
d
e


a
b
d
c
e

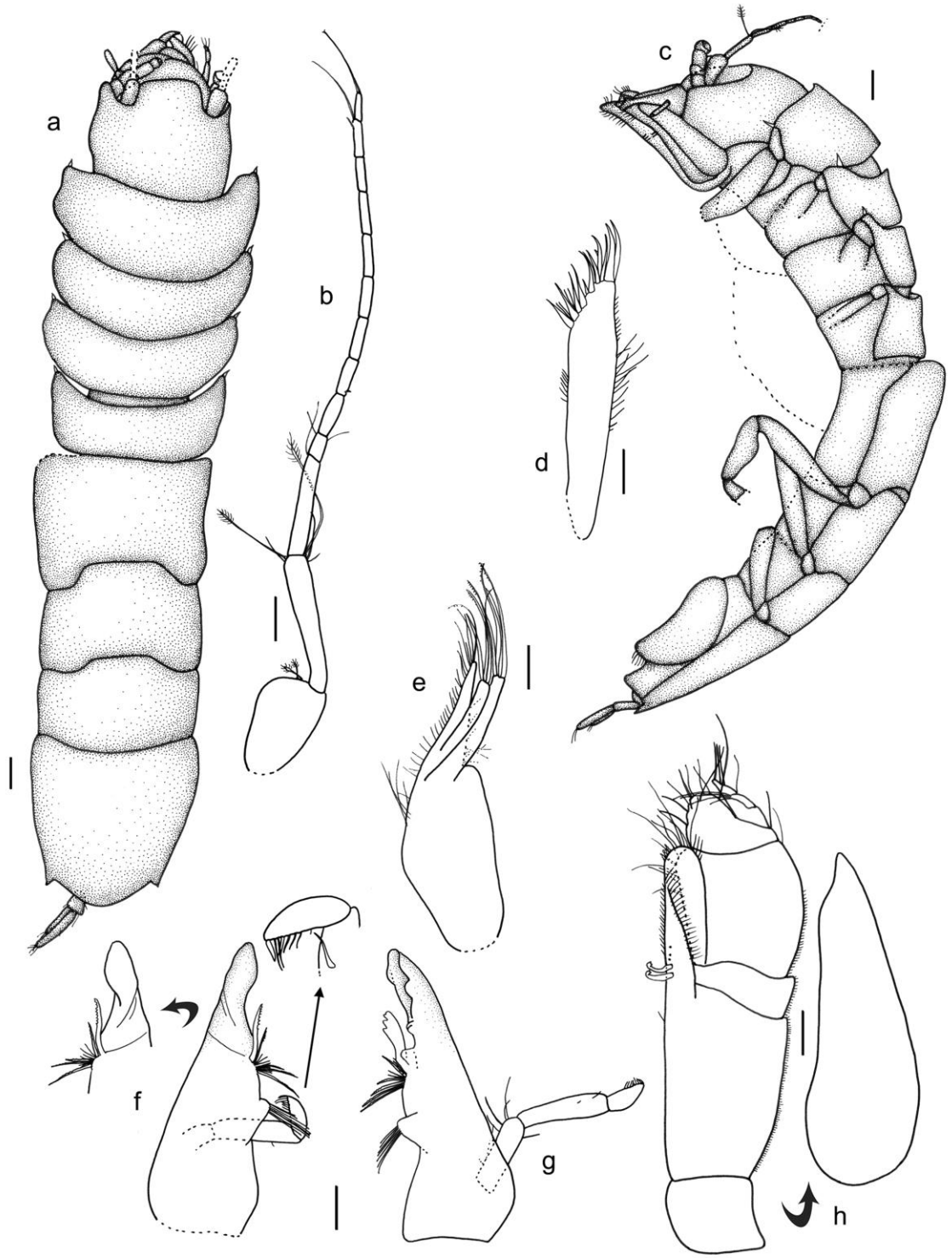
a
b
c
d
e
f
g
h

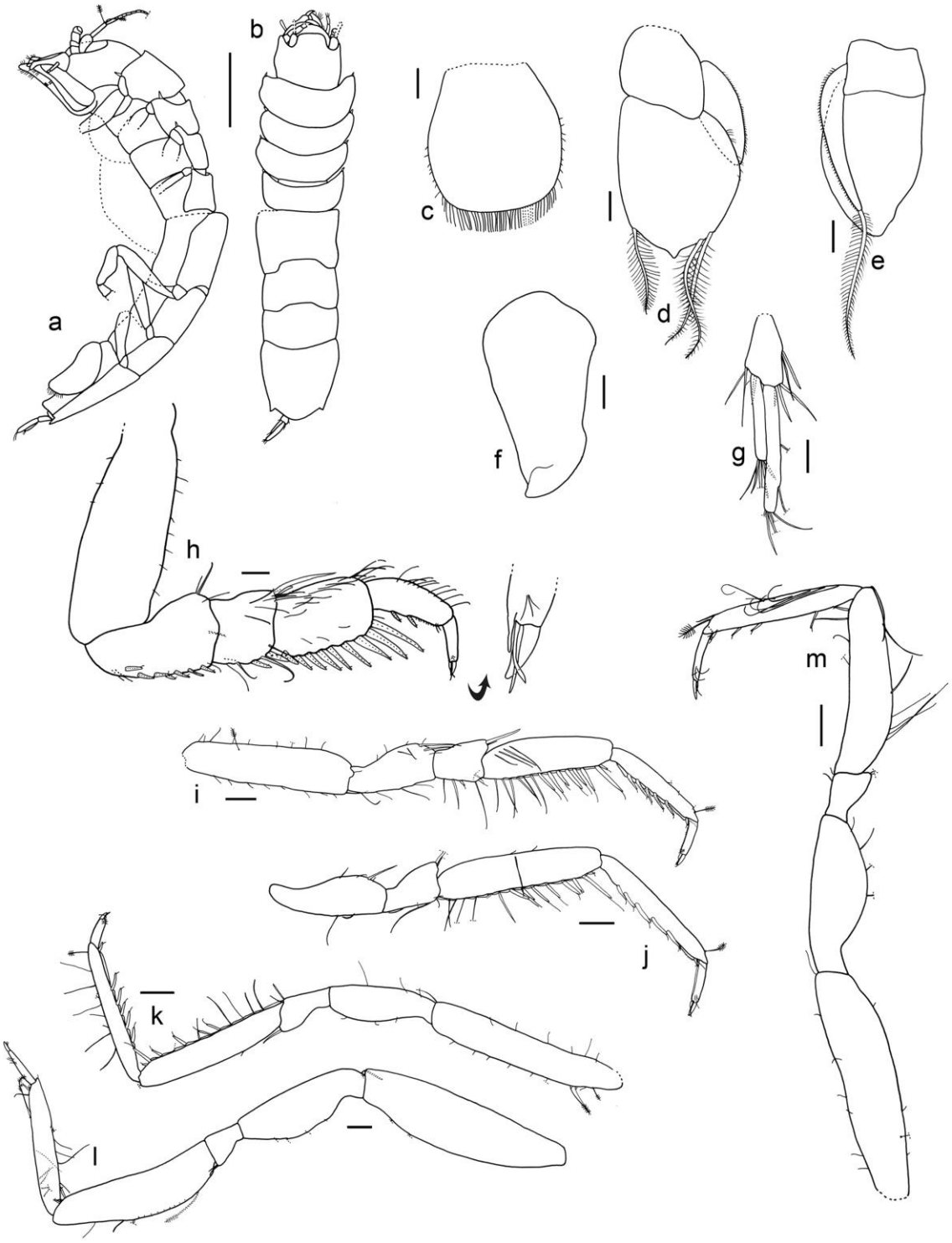
a
b
c
d
e
f
g
h
i
j
k
l
m

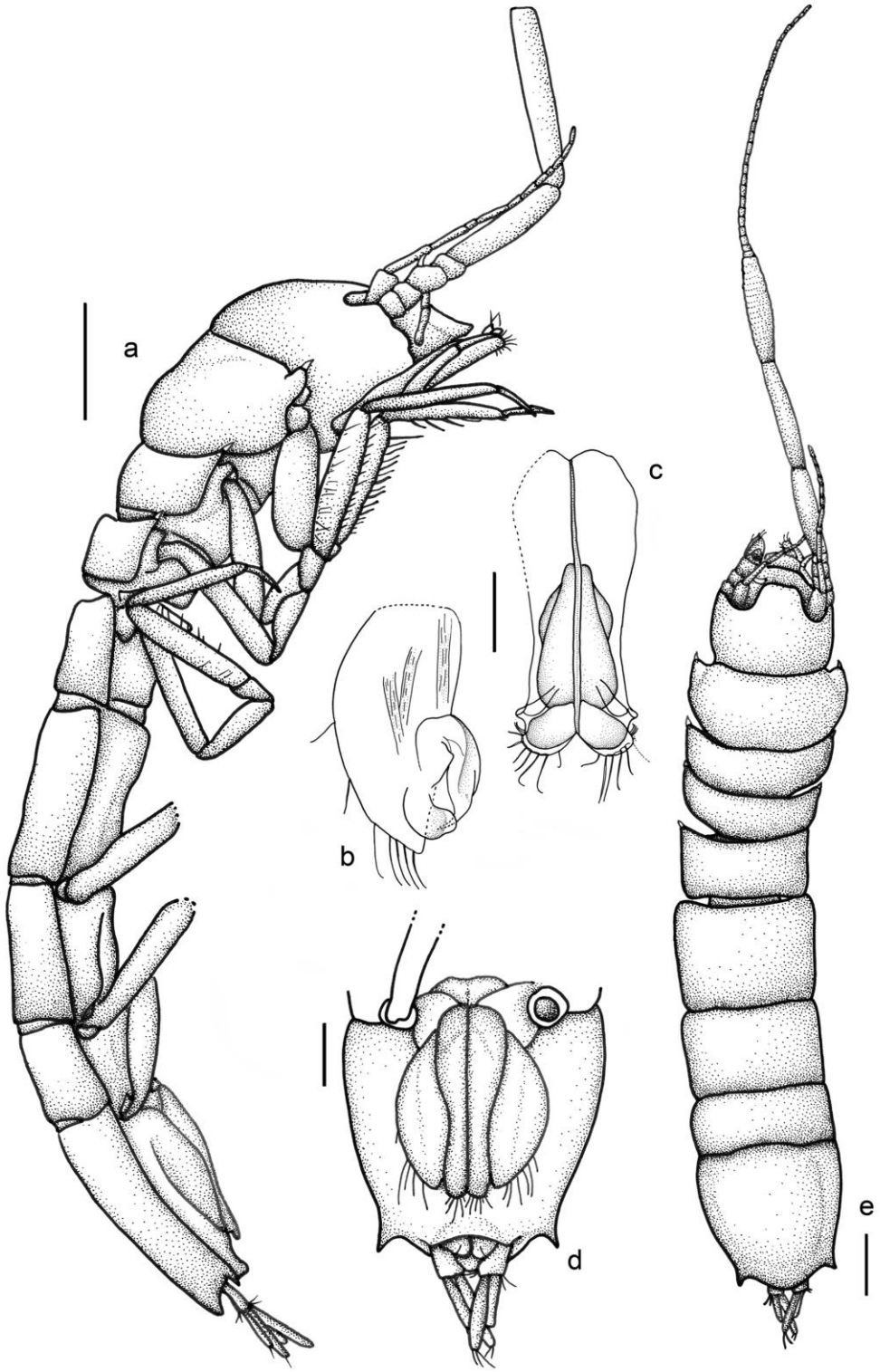
a
b
c
d
e


a
b
c
d
e
f

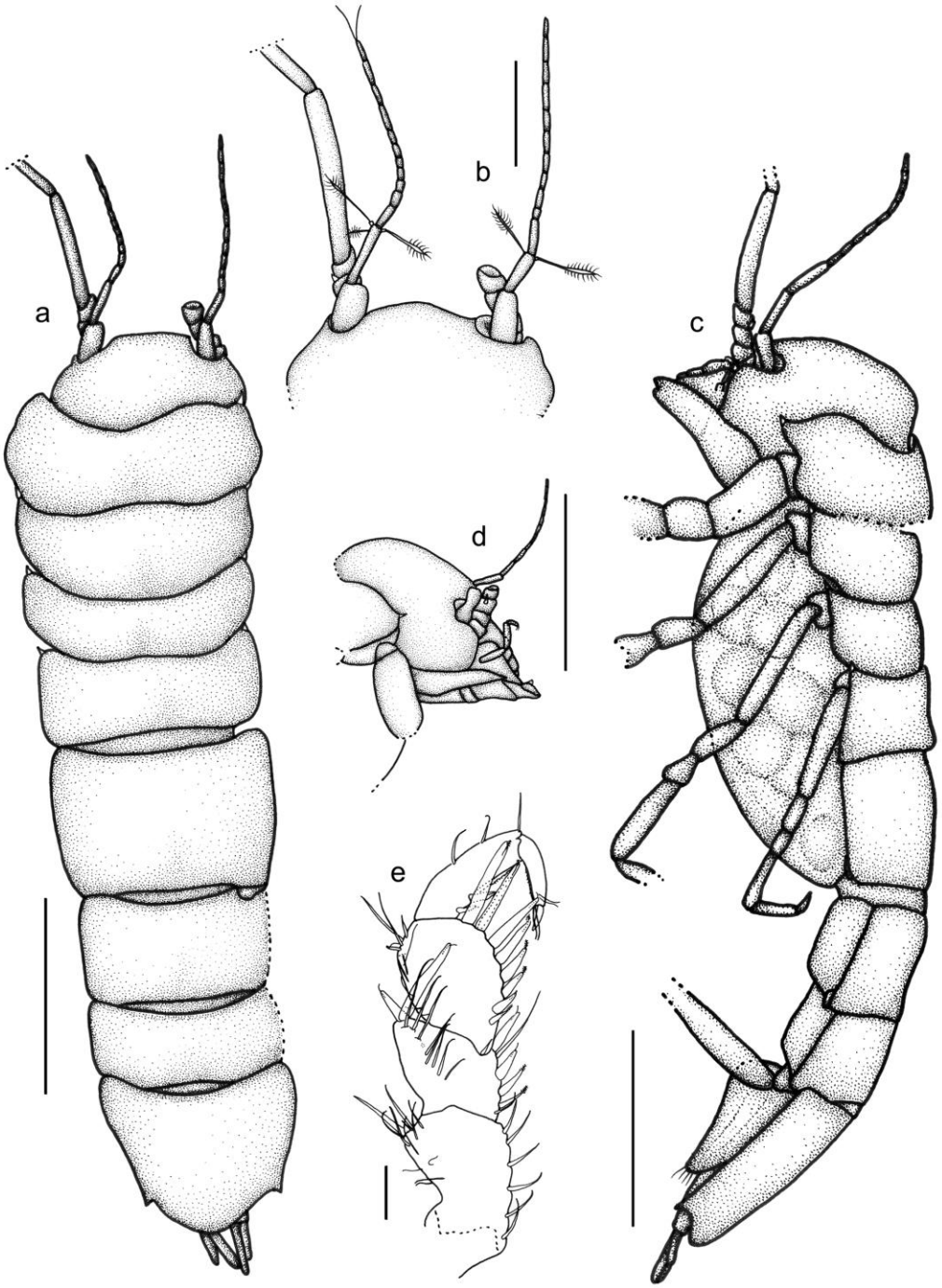
a
b
c
d
e

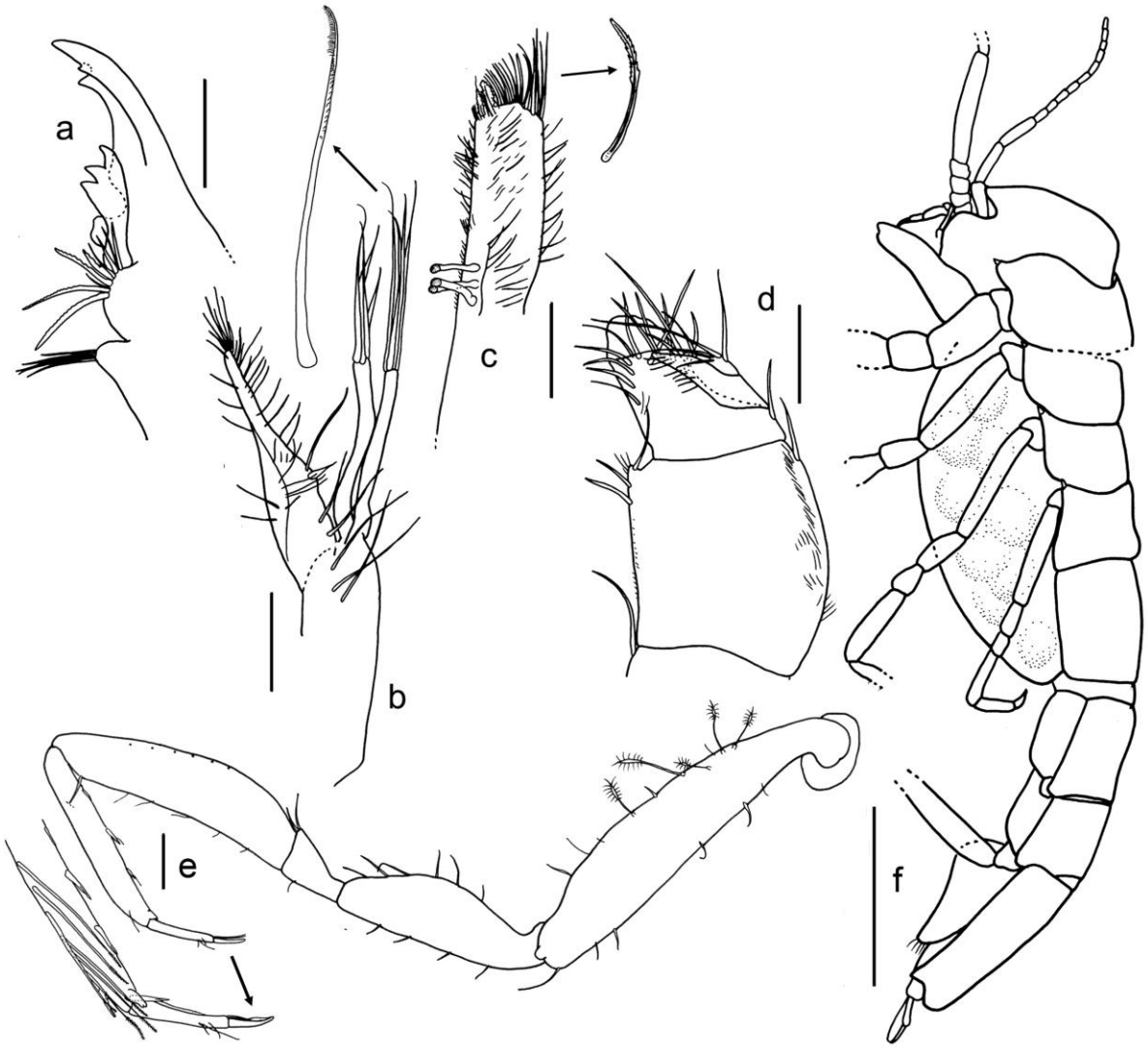
a
b
c
d
e
f

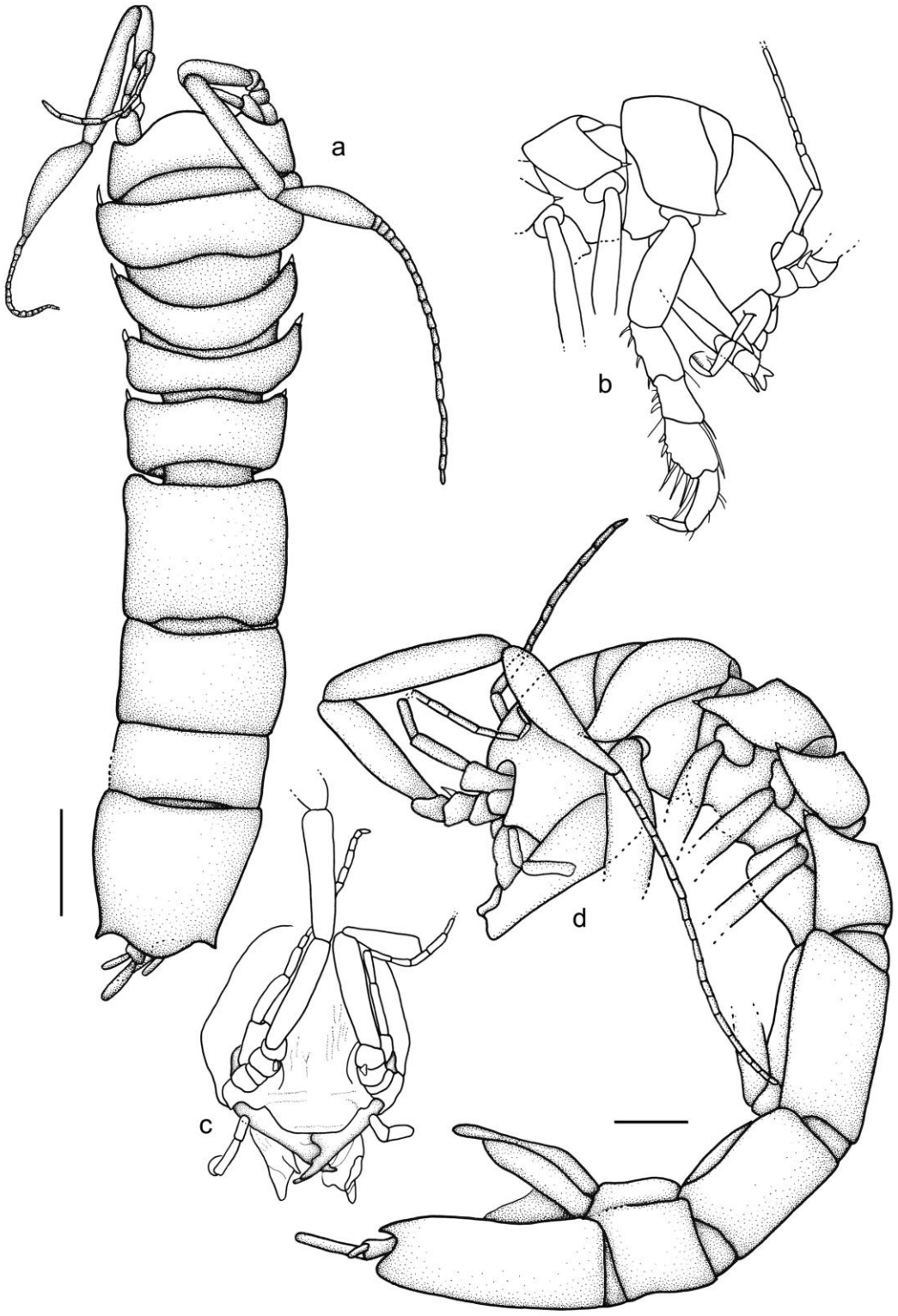
a
b
c
d

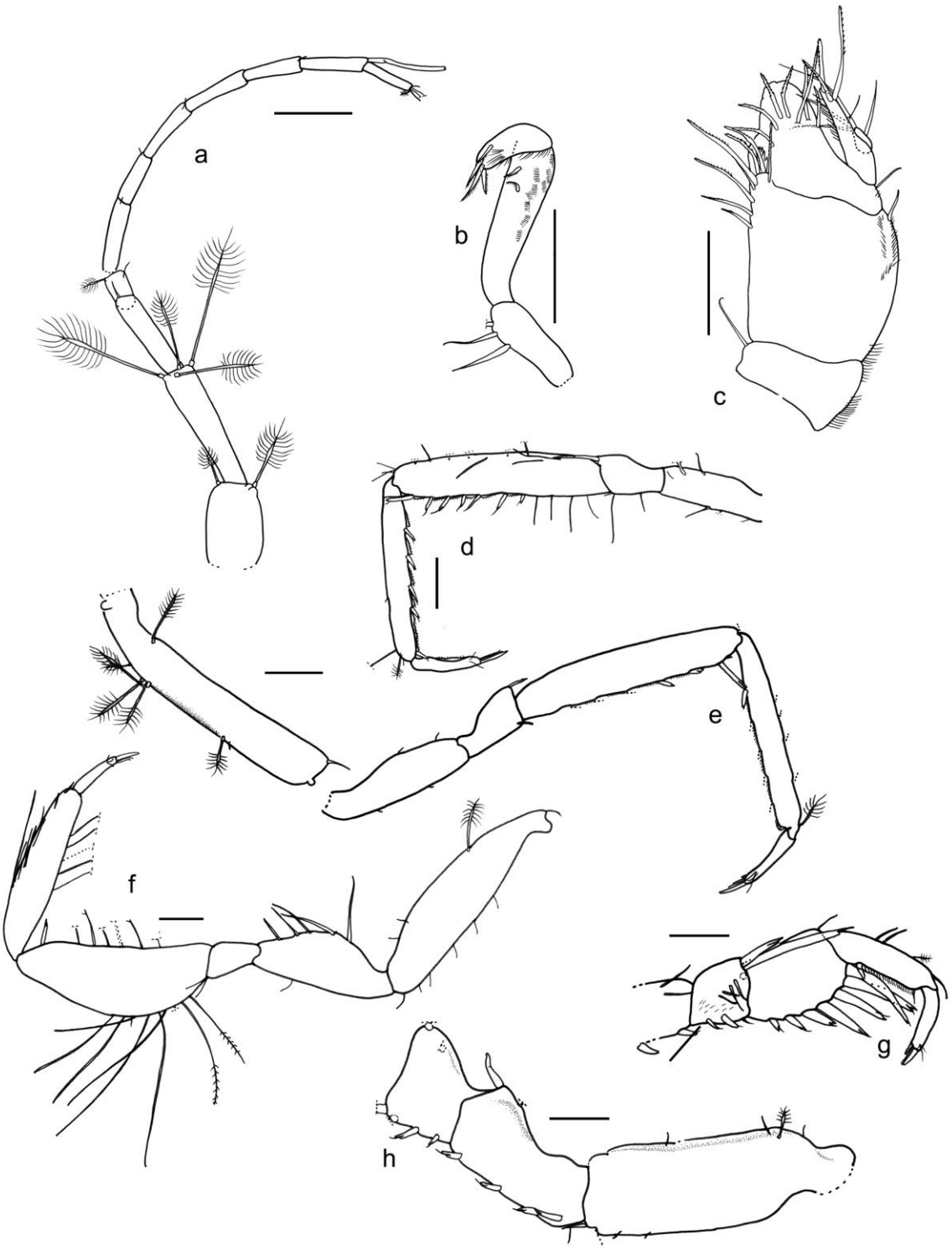
a
b
c
d
e
f
g
h


a
b
c
d
e
f

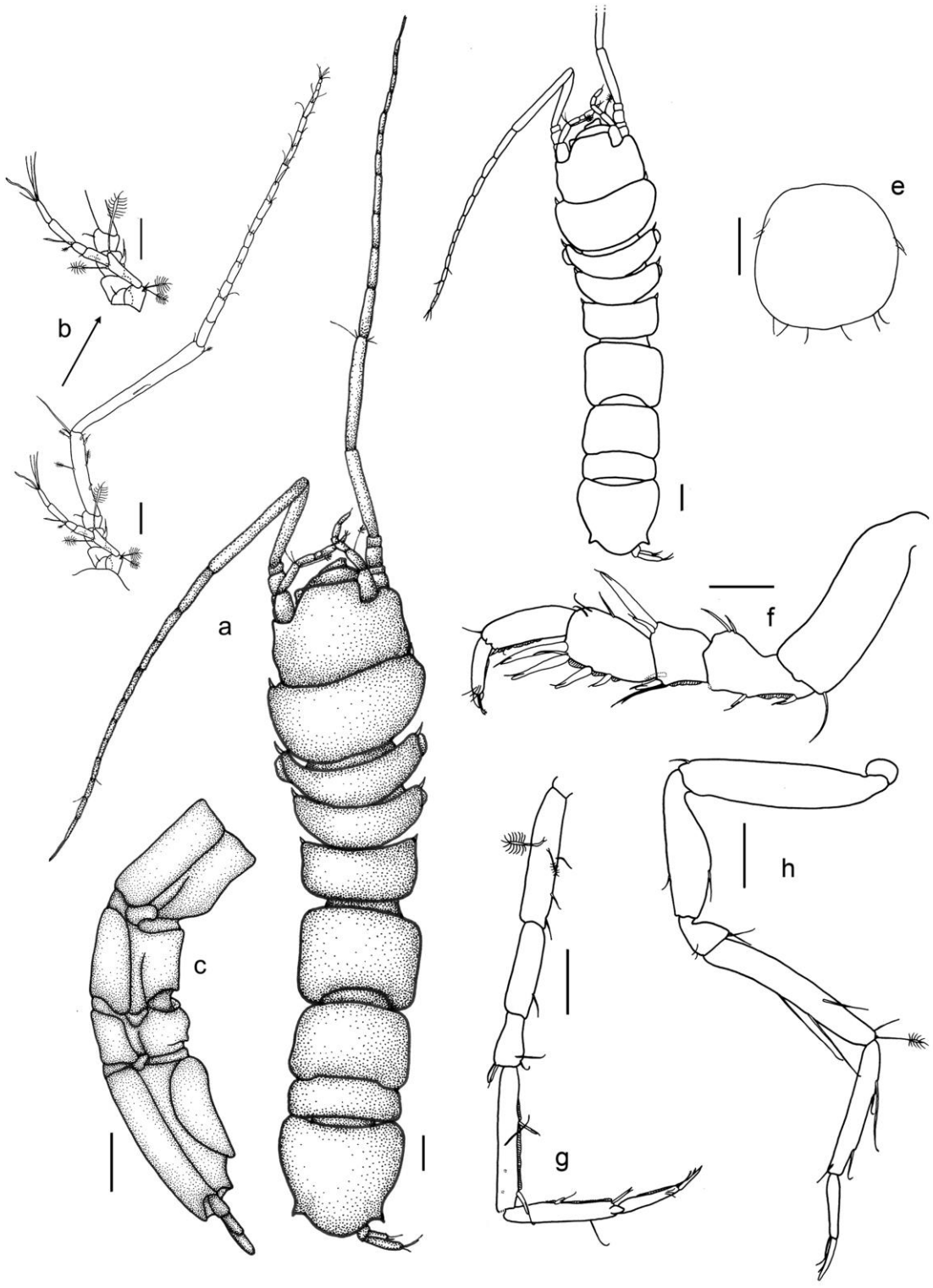
a
b
c
e
f
g
h


a
b